Gondwana Research 21 (2012) 378–393

Contents lists available at ScienceDirect

Gondwana Research

journal homepage: www.elsevier.com/locate/gr

Identification and isotopic studies of early Cambrian magmatism (El Carancho Igneous Complex) at the boundary between Pampia terrane and the Río de la Plata craton, La Pampa province, Argentina

Carlos J. Chernicoff [a,b,*], Eduardo O. Zappettini [b], João O.S. Santos [c,d], Marta C. Godeas [b], E. Belousova [e], Neal J. McNaughton [c]

[a] Council for Scientific and Technical Research (CONICET), Argentina
[b] Argentine Geological-Mining Survey (SEGEMAR), Argentina
[c] University of Western Australia, Australia
[d] Redstone Resources, Australia
[e] ARC National Key Centre for Geochemical Evolution and Metallogeny of Continents (GEMOC), Macquarie University, Sydney, Australia

ARTICLE INFO

Article history:
Received 17 November 2010
Received in revised form 25 February 2011
Accepted 5 April 2011
Available online 6 May 2011

Keywords:
Pampean magmatic arc–backarc
U–Pb SHRIMP
Hf isotopes
Aeromagnetics
La Pampa province

ABSTRACT

We have identified late Early Cambrian metaigneous rocks very poorly exposed at the Estancia El Carancho, in central La Pampa province, Argentina. They comprise calc–alkaline metadiorite and metagranite, and tholeiitic metapyroxenite and metagabbro. They are jointly referred to as the El Carancho Igneous Complex, and regarded to pertain to the Pampean magmatic arc and backarc, respectively. Titanite U–Pb SHRIMP dating of the metapyroxenite yielded 528 ± 5 Ma, and zircon U–Pb SHRIMP dating of the metadiorite yielded 520 ± 1.4 Ma. Hafnium isotope determinations on the dated zircons show $^{176}Hf/^{177}Hf$ ratios corresponding to positive εHf values from +7.18 to +9.37; Hf model ages of the Cambrian zircons yielded 884 Ma. It is interpreted that the metadiorites of the Complex crystallized from an Early Neoproterozoic (Tonian) juvenile source. We argue that the inferred occurrence of juvenile Tonian magmatic rocks in the (otherwise, mostly Paleo-Mesoproterozoic) substratum of the southern Pampia terrane could indicate a zone of thinned basement possibly associated with the early stage of Rodinia's breakup. In addition, the studied segment of the Pampean magmatic arc is contaminated by also juvenile, Late Mesoproterozoic crust, as evidenced by the presence of xenocrystic cores of 1140–1194 Ma – T_{DM}-Hf 1720 Ma and εHf values of +3.24 to +4.85 – in the Cambrian zircons, hence suggesting that the studied segment of the Pampean magmatic arc was intruded into juvenile Late Mesoproterozoic magmatic arc rocks. The El Carancho Igneous Complex would be located at the tectonic boundary between the Pampia terrane and the Río de la Plata craton. This boundary stands out in the aeromagnetic data as a change in the structural orientation about a roughly N-S line located approximately at 65° W and representing the suture zone between the Pampia terrane and the Río de la Plata craton. Our geotectonic model envisages westward dipping subduction of oceanic crust beneath the Pampia terrane; the El Carancho Igneous Complex would, therefore, have been originated on the Pampia side (upper plate) of the suture. Slivers of the arc- and backarc-type rocks would have been tectonically imbricated in the suture zone during the Pampean orogeny.

1. Introduction

The Neoproterozoic–Cambrian basement of south-central La Pampa province, Argentina, comprises the southernmost portions of the Pampia terrane and the Río de La Plata craton (Fig. 1), as established by Chernicoff and Zappettini (2004) on the basis of regional aeromagnetic data (SEGEMAR, 2005) and the study of the very limited basement outcrops exposed in the region (e.g. Chernicoff et al., 2010a; Zappettini et al., 2010).These data have permitted to identify lithologic, structural, geochronological and genetic differences between either basement block. Formerly, the basement rocks of this region were regarded to pertain to a single stratigraphic unit irrespective of terrane boundaries (Las Piedras Complex; Tickyj et al., 1999).

A roughly N-S trending linear feature that stands out in the aeromagnetic map of the region is regarded to depict the southernmost segment of the Pampia terrane/Rio de la Plata craton tectonic boundary; the magnetic fabric and foliation trend conspicuously N-S to NNE in the Pampia terrane, and NW to WNW in the Rio de la Plata Craton. In the close proximity of the suture, we have identified and dated late Early Cambrian metaigneous rocks, herein referred to as the El Carancho Igneous Complex. This Complex comprises calc–alkaline metadiorites and metagranites, as well as tholeiitic metapyroxenites

* Corresponding author at: Council for Scientific and Technical Research (CONICET), Argentina. Tel.: +5411-43493099; fax: 5411-43493171.
E-mail address: jchern@mecon.gov.ar (C.J. Chernicoff).

1342-937X/$ – see front matter © 2011 International Association for Gondwana Research. Published by Elsevier B.V. All rights reserved.
doi:10.1016/j.gr.2011.04.007

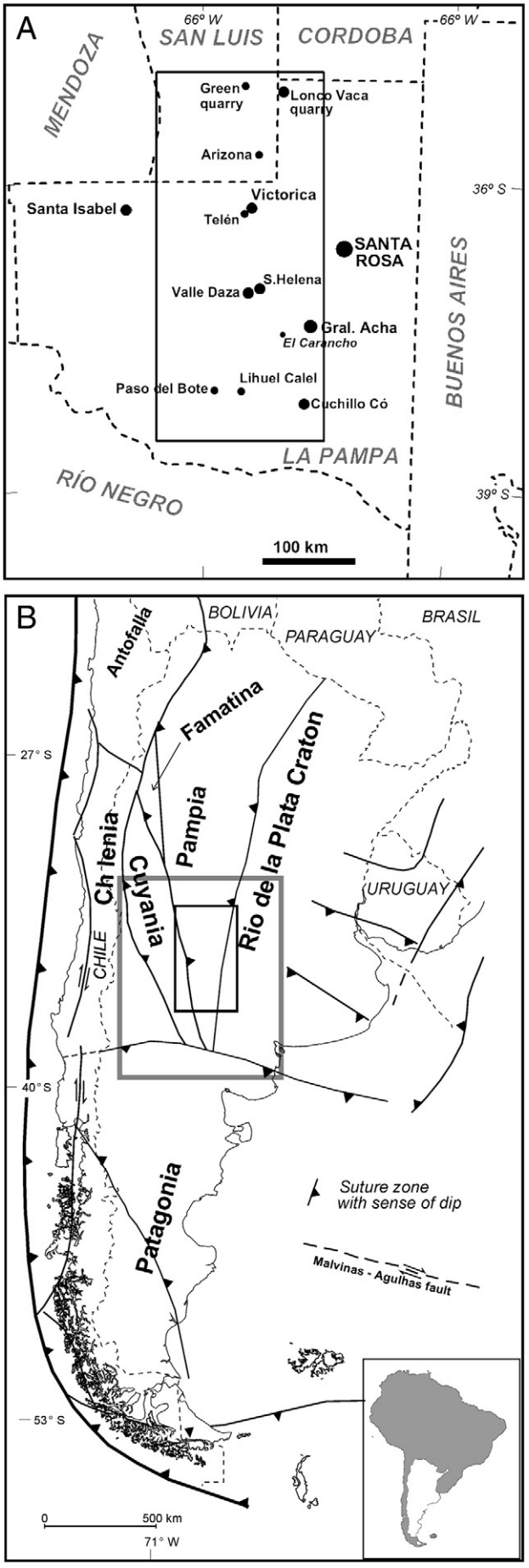

Fig. 1. a) Locality map of the study area (inner rectangle: geophysical coverage; see Fig. 2) and surrounding provinces of south-central Argentina. b) Study area and greater region in the context of the map of accreted terranes in southern South America. Slightly modified after Chernicoff and Zappettini, 2004.

and metagabbros, both being very poorly exposed at the El Carancho estate, possibly as roof pendants in a Silurian granitoid (Fig. 2d). The scattered outcrops are individually smaller than 1 m^2, occurring along the ground around and nearby the El Carancho salt pan (65°04′ W–37°27′ S). Locally they are also found as xenoliths in the Silurian granitoid and related pegmatites exposed south of the El Carancho estate (65°10′ W–37°34′ S).

In the present study we describe the lithologies of the Complex and present U–Pb SHRIMP dating on zircons and titanites from the metadiorites and metapyroxenites, respectively, as well as Hf isotope determinations on the dated zircons and geochemical data. We also include the interpretation of the imaged regional geophysical data (aeromagnetics and gravity) of the study area for a better understanding of the geological and structural framework (Fig. 2d).

The results are interpreted within the context of the Neoproterozoic–Cambrian evolution of the southwestern margin of Gondwana, focusing on the significance of the El Carancho Igneous Complex as the southernmost expression of the Pampean magmatic arc. The Discussion deals with the juvenile character of the Complex, its relationship with the Brasiliano magmatism, the post-Pampean evolution of the region, and the configuration of the Río de la Plata craton and the Pampia terrane.

2. Geological framework: Río de la Plata craton and Pampia terrane

The Rio de la Plata Craton of southern South America is considered to encompass autochthonous Archean to Palaeoproterozoic Gondwana basement (e.g. Cordani et al., 2000; Santos et al., 2003; Dalla Salda et al., 2005, and references therein; Spagnuolo et al., 2011). Some workers (Schwartz and Gromet, 2004; Rapela et al., 2007) have argued about its 'exotic' nature in relation to its present-day neighboring Neoproterozoic to Cambrian basins, although this criterion has been found not to be applicable to the northern and central segments of the Proto-Andean margin (Chew et al., 2008); also, the identification of abundant Mesoproterozoic detrital zircons in the Neoproterozoic supracrustal sequences on the core of the craton (Gaucher et al., 2008) points to the Rio de la Plata craton, rather than to the Kalahari craton, as their most likely provenance (see Discussion: The configuration of the Río de la Plata craton, below).

The Pampia terrane is regarded to comprise the Precambrian–Early Paleozoic metamorphic basement of the eastern Sierras Pampeanas located to the west of the Rio de la Plata Craton. Different viewpoints have been proposed for this terrane, including e.g. its allochthonous nature and late Proterozoic collision with the Río de la Plata craton (Kraemer et al., 1995; Ramos, 1988), or its para-autochthonous character and Early Cambrian collision with the Río de la Plata craton (e.g. Rapela et al., 1998). Ramos et al. (2010) envisage it as being a large cratonic block of Rodinia's attached to the Amazon craton since the Mesoproterozoic, jointly colliding with the Paranapanema block during the Neoproterozoic, and finally colliding with Río de la Plata craton during Early Cambrian. Our concept about Pampia (and the Río de la Plata craton) is discussed in Section 7.4, below (see also Chernicoff et al., 2010c).

No pre-Neoproterozoic basement rocks are exposed in this region. However, Hf isotope evidence indicates that the unexposed pre-Neoproterozoic basement of southern Pampia encompasses both reworked Paleo–Mesoproterozoic and juvenile Mesoproterozoic components. Evidence includes: a) Hf isotope determinations on dated detrital zircons from Neoproterozoic–Lower Paleozoic cover sequences, e.g. La Horqueta Formation (Chernicoff et al., 2008d), Santa Helena Schist (Zappettini et al., 2010) and Green Schist

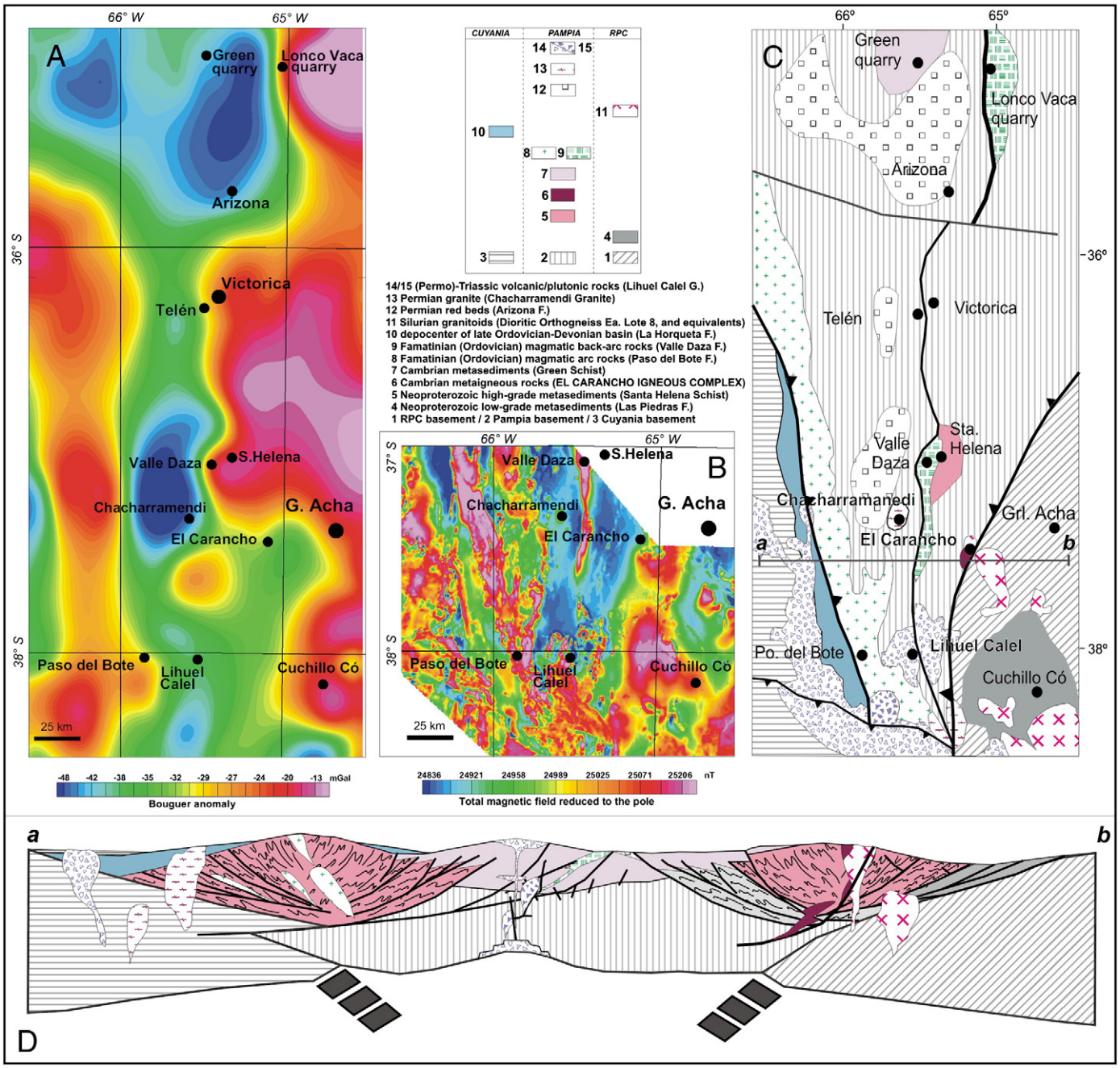

Fig. 2. Geophysical data of the study region (A: gravimetric data; B: aeromagnetic data; see location in Fig. 1), basement geology of the study region (C) based on limited exposures and geophysical data, and E–W geologic section at 37°30′S (*ab* in basement map; D). Note: there are no aeromagnetic data to the north of 37°S.

(Table 4), and b) Hf isotope data on magmatic zircons from Lower Paleozoic magmatic units, e.g. Paso del Bote Formation (Chernicoff et al., 2010a), Valle Daza Formation (Chernicoff et al., 2011a,b) and El Carancho Igneous Complex (this article). The proportion of reworked Paleo-Mesoproterozoic and juvenile Mesoproterozoic components cannot yet be fully evaluated, but both would be present as part of a continental crust forming the actual substratum of the Puncoviscana Basin.

The post-Mesoproterozoic basement stratigraphy of the study area and broader region is synthesized in the map presented in Fig. 2c, which is based on the limited exposures available and on geophysical information (Fig. 2a and b).

The oldest rocks of the region are supracrustal rocks formed in a platform environment on the Rio de la Plata Craton, represented by the low-grade metasedimentary rocks exposed at Cuchillo Có and surroundings (Las Piedras Formation: mostly metapelites and metapsammites, and minor quartzite and marble). Recent U–Pb SHRIMP dating of Las Piedras Formation metapelites have yielded ca. 555 Ma (Chernicoff et al., 2010b), whereas the Ar–Ar age of metamorphism was previously established at ca 523 Ma (Tickyj et al., 1999). Unlike the roughly coeval upper-plate sediments represented by the Santa Helena Schist (Zappettini et al., 2010), the Las Piedras Formation was not affected by the subsequent Famatinian (Middle Ordovician) metamorphism. The Las Piedras Formation may possibly be partly equivalent to the Neoproterozoic–Early Cambrian platform sequences of the Rio de la Plata craton exposed in Tandil, i.e. Sierras Bayas Group/Cerro Negro Formation (e.g. Poiré and Spalletti, 2005; Gómez Peral et al., 2007), and in Uruguay, i.e. Arroyo del Soldado

Group (e.g. Gaucher et al., 2005). The Las Piedras Formation is intruded by Silurian granitoids — Estancia Lote 8 Dioritic Orthogneiss dated at ca 432 Ma (zircon U–Pb SHRIMP data; Chernicoff et al., 2011b), coeval with the nearby Andersen Granodiorite dated at 431 ± 12 Ma, U–Pb in zircon (Tickyj et al., 1999), that cut the NW- to WNW-trending structural fabric of the Rio de la Plata craton (Chernicoff and Zappettini, 2004).

Neoproterozoic to Early Cambrian metasedimentary units, limited to the Pampia terrane, are represented by minor outcrops grouped in the Santa Helena Schist and the Green Schist. The first one represents a metamorphic unit whose protolith was deposited after ca. 556 Ma and prior to ca. 530 Ma in a foreland basin possibly equivalent to the late Puncoviscana basin (Zappettini et al., 2010). Cambrian metasedimentary rocks are grouped in the Green Schist, whose protolith was deposited after ca. 500–515 Ma and prior to ca. 465 Ma (Chernicoff et al., 2007, 2008b) in a post-collisional basin (mostly sourced from the Pampean orogen), slightly postdating Middle- to Late Cambrian sedimentation that occurred in more northern latitudes (e.g. syn-collisional Negro Peinado and Achavil Formations (Collo et al., 2009)).

The collision between the Pampia terrane and the Rio de la Plata craton would have been preceded by west dipping subduction of oceanic crust (i.e. consumption of the Pampean ocean) and juvenile arc and back-arc arc magmatism developed on the Pampia terrane (upper plate). The very scarce exposures of slivers of both rock types, identified by the authors in La Pampa province, Argentina, have been grouped in the El Carancho Igneous Complex, and are interpreted to be tectonically imbricated in the suture zone. The occurrence of Pampean intrusives on the Pampia terrane side of the Pampia terrane/Rio de la Plata craton suture coincides with the gravimetric model of the Sierras Pampeanas of Córdoba at latitude 31° 05′S (Ramé and Miró, 2010), where the Ascochinga Igneous Complex (equivalent to the "G1a" metaluminous granitoits of Rapela et al., 1998, dated at ca 530 Ma) is placed on the Pampia terrane side of the suture, hence representing its upper plate. The envisaged westward slab polarity (also indicated by Trindade et al., 2006) differs from the eastward slab polarity proposed in previous models of the Pampean Orogen (see e.g. Rapela et al., 1998). To the north of the Sierras Pampeanas, the eastern border of Arequipa–Antofalla/Pampia would have been the active margin, and the Rio Apa cratonic fragment (i.e. southern extension of Amazonia; Santos et al., 2008) would have been the passive margin, this scheme being consistent with the occurrence of Early Cambrian arc magmatism in northwestern Argentina (Zappettini et al., 2010).

Both the Santa Helena Schist and the Green Schist are the host rocks of Ordovician metaigneous rocks that pertain to the southernmost Famatinian arc (Paso del Bote Formation; metaquartz-diorites and associated rocks dated at ca. 466–476 Ma; Chernicoff et al., 2010a) and backarc (Valle Daza Formation; metagabbros dated at ca. 450 Ma; Chernicoff et al., 2008c, 2009). Both Famatinian rock assemblages define narrow, roughly N-S trending belts.

3. Regional geophysics

Chernicoff and Zappettini (2004) firstly reported the tectonic features identified in the aeromagnetic survey of La Pampa province in the broader context of the southern-central region of Argentina, depicting the configuration of the southern portions of the Chilenia, Cuyania and Pampia terranes, as well as that of the Rio de la Plata craton, all of them terminating at the northern boundary of the Patagonia terrane (see also Fig. 1b).

Additional ground truthing of the aeromagnetics (and more limited gravimetric data), as well as laboratory work, has focused the attention on each of the tectonic boundaries, their associated rock assemblages and their geophysical responses (Chernicoff and Zappettini, 2007; Chernicoff et al., 2007, 2008d, 2009; Zappettini et al., 2010).

Unlike the Pampia/Cuyania suture, where both terranes exhibit roughly N-S trending structures detected by aeromagnetics, the Pampia/Río de la Plata craton boundary involves a change in the structural orientation, which occurs about a roughly N-S line located approximately at 65° W. On the western (Pampia) side of the bounding line, the structural fabric trends roughly N-S, whereas immediately east of this boundary (i.e. Río de la Plata craton), the structural fabric trends NW to WNW. On both sides of the Pampia/Río de la Plata craton boundary line, the structural pattern of the basement is partially obliterated by younger magmatic rocks (Silurian granitoids, Permo-Triassic magmatic rocks) which, nevertheless, do not preclude detecting the major Pampia/Río de la Plata craton boundary (Fig. 2).

Towards the north of the study region, the Pampia/Río de la Plata craton boundary is hidden under the sedimentary and volcanic rocks of the Paraná basin, where no aeromagnetic data are available (and the scattered gravimetric data are not helpful). At about 32°S, the Pampia/Río de la Plata boundary has been inferred from east–west magnetotelluric and gravimetric profiles (Booker et al., 2004, and Ramé and Miró, 2010, respectively).

To the south of the present study area, the Pampia/Río de la Plata boundary is regarded not to extend any further south than about 39°S, where there is a large-scale, roughly E–W magnetic and gravimetric anomaly thought to represent the northern margin of the Patagonia terrane (Fig. **5**, in Chernicoff and Zappettini, 2004; see also seismic data of Mosquera and Ramos, 2006).

A geological interpretation of the aeromagnetic (and gravimetric) survey of the greater study area helped drawing a basement geological map of the region, presented in Fig. 2c. In addition to the broader terrane boundaries between the Río de la Plata craton, Pampia and Cuyania (1 to 3, in Fig. 2c), the main units delineated in this map are: (4): Upper Neoproterozoic–Early Cambrian metasediments of the Río de la Plata craton (Las Piedras Formation); (5): Upper Neoproterozoic–Early Cambrian metasediments of Pampia (Santa Helena Schist); (6): Early Cambrian metaigneous rocks associated with the Pampia/Río de la Plata craton suture (El Carancho Igneous Complex; this article); (7): Cambrian metasedimentary rocks of Pampia (Green Schist); (8): Ordovician magmatic arc rocks (Paso del Bote Formation); and (9): Ordovician magmatic back-arc rocks (Valle Daza Formation). Also, for the sake of completion, the map depicts the outcrops (and interpreted suboutcrops) of: (10): Upper Ordovician to Devonian marine foreland deposits (La Horqueta Formation, sitting on Cuyanian basement; these sediments are geophysically undistinguishable from a small patch of overlying Permian sediments of the Carapacha Formation); (11): Silurian granitoids (Dioritic Orthogneiss of Estancia Lote 8, and equivalents); (12): Permian red beds (Arizona Formation); (13): Permian granite (Chacharramendi Granite); (14/15): (Permo)-Triassic volcanic and plutonic rocks (Lihuel Calel Group/Estancia El Trabajo Stock). An E–W geologic section of the basement map at 37° 30′ S is shown in Fig. 2d.

It should be noted that the metadiorites and metagranites of the El Carancho Igneous Complex (located in the immediate western proximity of the Pampia/Río de la Plata craton boundary), show almost no magnetic contrast with the surrounding metasedimentary rocks (Santa Helena Schist, Green Schist), which precludes their precise delimitation. As regards the metapyroxenites and metagabbros of the Complex, although their magnetic susceptibility is much higher than that of the metasedimentary rocks (2.324×10^{-3} SI, as opposed to 0.363×10^{-3} SI), the absence of a pronounced magnetic anomaly would be indicative of their very small volume, herein interpreted as small slivers of upthrust material (see Discussion, below).

4. Petrological and geochemical characteristics

The metaigneous rock types identified in the El Carancho Igneous Complex comprise two lithologic groups that will be described separately: a tholeiitic suite with MORB affinities and a calc–alkaline

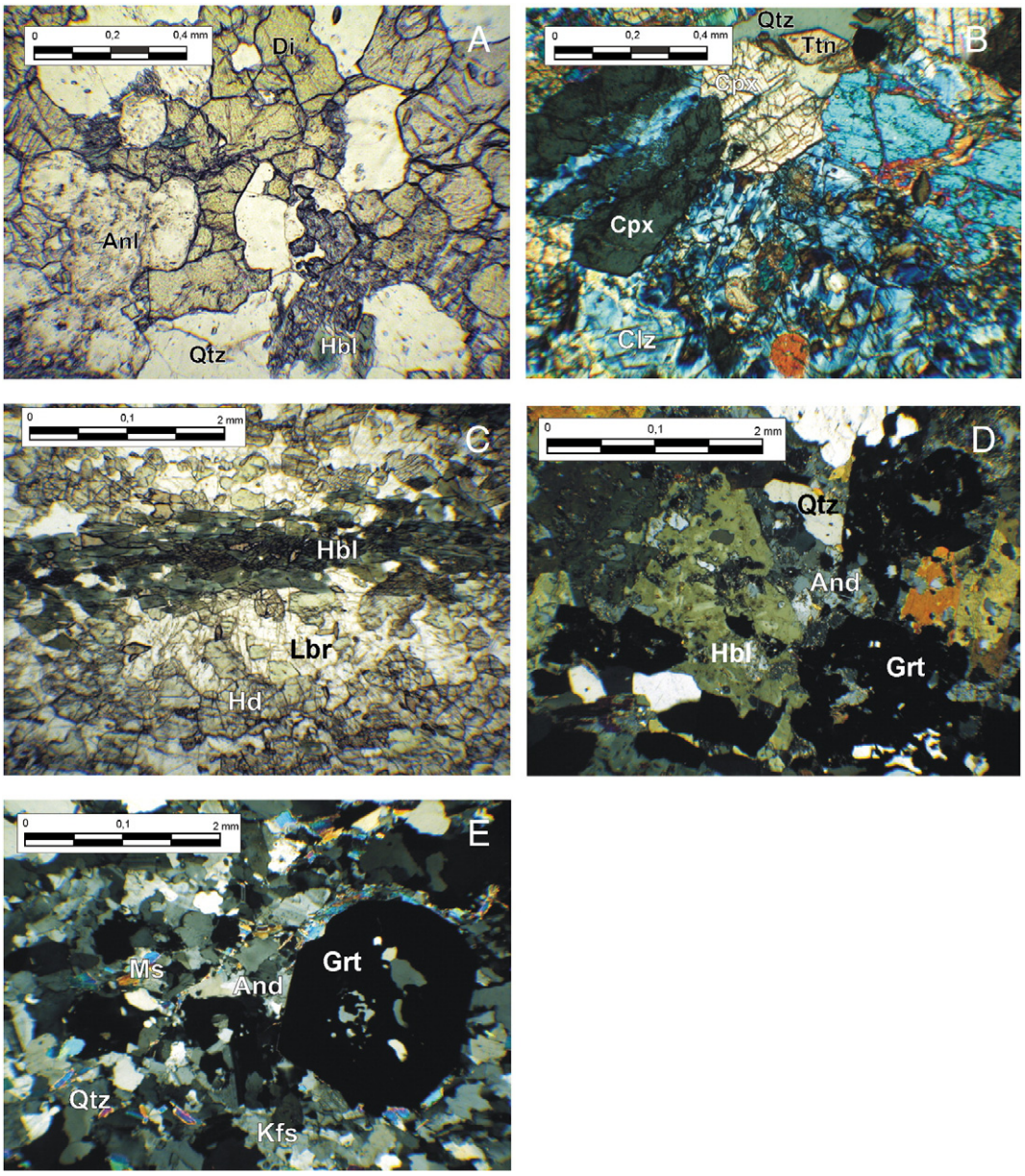

Fig. 3. Photomicrographs illustrating relictic igneous lithologies and metamorphic assemblages of the El Carancho Igneous Complex, La Pampa. a) Meta-analcime gabbro, b) Metapyroxenite, c) Metagabbro, d) Metadiorite, e) Metagranite. Reference: And: Andesine. Anl: Analcime. Clz: Clinozoisite. Cpx: Clinopiroxene. Di: Diopside. Grt: Garnet. Hbl: Hornblende. Hd: Hedenbergite. Kfs: Potassic feldspar. Lbr: Labradorite. Qtz: Quartz. Ttn: Titanite.

arc suite (Chernicoff et al., 2009). A local variety classified as meta-analcime gabbro (metateschenite) is regarded as a precursor of the tholeiitic back-arc magmatism.

The rocks of the Complex reached amphibolite-facies regional metamorphism, represented by the hornblende–plagioclase association (locally, there is evidence of metamorphism in the granulite facies); granoblastic texture and foliation were developed at this stage. This was followed by ductile deformation under greenschist-facies conditions with neoformation of clinozoisite replacing clinopyroxene. Finally, under brittle conditions microfracturing took place, represented by planes of cataclasis often filled with quartz and calcite.

Fig. 4. Major and trace element composition diagrams of the El Carancho Igneous Complex rocks. a): AFM diagram. Boundary between the calc–alkaline and the tholeiitic fields after Irvine and Baragar (1971); dashed line (tholeiitic trend) after Macdonald and Katsura (1964); field of tholeiites (hatched area) after Bailey and Blake (1974). Also shown are magmatic rocks from the Pampean Arc from Córdoba (gray areas; after Lira et al., 1997). References: solid circle: metagabbro; empty circle: metapyroxenite; triangle: metadiorite; square: metagranite. b): Ti–Zr plot of the basic metaigneous suites. References: see Fig. 4a. U–Pb SHRIMP dated samples are indicated. MORB: Middle Ocean Ridge Basalts; VAB: Volcanic Arc Basalts. c): E-Type MORB normalized multielement pattern of the tholeiitic rocks. References: gray area: metapyroxenite; hatched area: metagabbro. d): Chondrite-normalized REE concentration patterns (normalizing values from Taylor and McLennan, 1985) of the tholeiitic rocks. References: see Fig. 4c. e): Zr/4-Nb*2-Y discriminant diagram showing the metagabbros and metapyroxenites grouped in the MORB field. References: see Fig. 3. AI and AII = Intraplate alkali basalts; AII and C = Intraplate tholeiites; B = P-MORB (Middle Ocean Ridge Basalts); D = N-MORB; C and D = Volcanic Arc basalts. f): Cr versus Y diagram showing the MORB field, plots of the tholeiitic rocks, and percentage of melting (after Pearce, 1982) of the source from which the mafic magma was derived. References: see Fig. 4a. g): E-Type MORB-normalized multielement pattern of the calc–alkaline rocks. References: Solid line: metadiorite; hatched area: metagranite. h): Chondrite-normalized REE concentration patterns (normalizing values from Taylor and McLennan, 1985) of the calc–alkaline rocks. References: see Fig. 4g.

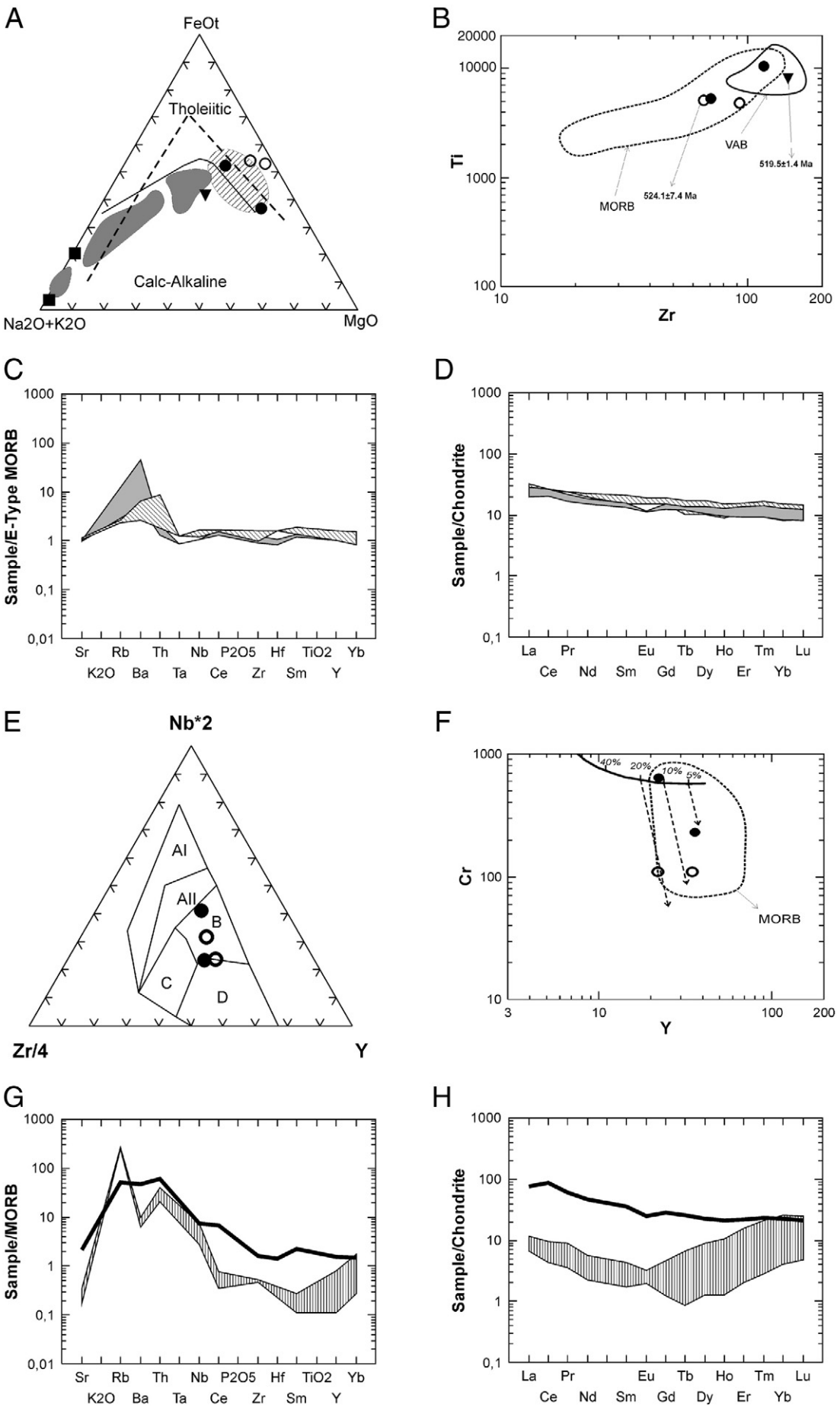

4.1. Tholeiitic suite and related rocks

4.1.1. Meta-analcime gabbro

This rock has brownish gray color. Suboriented mafic and leucocratic minerals can be observed at hand samples, as well as scarce white parallel veinlets of 3 mm width. The texture is banded granoblastic, due to bands composed of differential concentration of minerals; the components are calcic minerals, i.e. plagioclase (medium labradorite) and clinopyroxene (diopside). The association is completed by scarce analcime (Fig. 3a; identification of diopside and analcime were confirmed by X-ray diffraction analyses). Labradorite has slightly curved albite and albite-Carlsbad twinning, fractures and minor clay alteration. It is replaced by pistacite as grains and veinlets, and by a mica mineral (sericite?). Diopside is very fractured, and partially replaced by chlorite–serpentine material. Analcime is present as pseudocubic individuals with slight clay alteration; the pseudocubic habit would suggest that this mineral is a replacement product of leucite. Titanite, apatite and zircon complete the mineralogy. Ore minerals are very scarce. There is abundant, secondary quartz with fragmental extinction, scarce fractures and aligned fluid inclusions. It is interpreted that this rock is an alkaline gabbro or teschenite which has undergone high grade regional metamorphism in granulite facies, and late quartz injection that does not belong to the original igneous paragenesis.

4.1.2. Metapyroxenite

The metapyroxenites are whitish gray colored and fine grained. They exhibit coarse-grained blastograiny texture, relictic of grain texture affected by medium- to low-grade regional metamorphism (Fig. 3b). The principal component comprises diopside, with titanite as an accessory mineral. Clinopyroxene is partially transforming to clinozoisite; the epidote replaces the clinopyroxene that remains only as isolated relicts. Original calcic plagioclase was totally transformed into clinozoisite; its presence in the igneous protolith is evidenced by 40% anorthite ($Ab_{3-13}An_{87-97}$) in the norm (cf. Table 1, see Supplementary Data). The magmatic titanite (see Section 6.1.2.2., below), that has calcium in its composition and is present in a proportion that reaches 5–10%, is consistent with the calcic mineral paragenesis. Lesser amounts of quartz, either as individuals or as lense-like aggregates complete the mineralogy; the presence of quartz is in accordance with the 4.79–8.34% SiO_2 in the norm.

4.1.3. Metagabbro

The protolith was transformed into banded amphibolite, with a blastograined to granoblastic texture, where the original igneous characteristics persist locally (Fig. 3c). The main minerals are amphibole, clinopyroxene, plagioclase and very scarce quartz, with titanite as an accessory mineral. The banding is due to the existence of differential mineral concentration, resulting in alternating plagioclase-clinopyroxene and amphibole bands. Amphibole is hornblende, with a pleochroism varying from clear yellowish green to intense slightly bluish green. Hornblende is subidioblastic to xenoblastic, and presents an incipient gradual transformation to brown biotite and scarce pleochroic halos produced by minute inclusions of metamictic minerals. It is found as isolated individuals, as monomineral bands and as a product of the transformation of pyroxene. Pyroxene is a hedenbergite relic of the original rock of gabbroic composition. It is fractured, and it is found as a partial, incipient to moderate gradual pass to hornblende due to metamorphism. Plagioclase (labradorite) is xenoblastic; it has albite-Carlsbad and pericline twins; it shows incipient albitization and slight alteration to clays, epidote and sericite. Quartz is xenoblastic and it is found in a very scarce proportion. It shows locally poikilitic texture, including other mineral components. Titanite keeps the original igneous characteristics.

4.2. Calc–alkaline suite

It comprises metadiorite and metagranite.

4.2.1. Metadiorite

The metadiorites–metamonzodiorites are dark rocks, coarsely foliated, which under the microscope exhibit medium-grained blastograiny texture, as a relict of a grainy texture, which became diffuse because of the regional metamorphism and lesser cataclasis. The essential components include hornblende, quartz, plagioclase and potassic feldspar, the accessory minerals being garnet, titanite, zircon, allanite and tourmaline (Fig. 3d). Hornblende is the most abundant mineral; it forms very well developed megablasts with poikiloblastic texture due to plagioclase and quartz inclusions. Its pleochroism varies from clear green to intense green. It probably is a total transformation product of a preexistent pyroxene. Locally the gradual pass from hornblende to brown biotite is noted. Quartz appears as individuals or aggregates; it also constitutes bands which possibly have penetrated the rock under fragile conditions. Plagioclase is a basic andesine with scarce albite-Carlsbad twins. K-feldspar is present as grains with scarce perthites and Carlsbad twins. Garnet makes well-developed poikiloblasts that include quartz, titanite and zircon; it is fractured and scarce compared to the other minerals. Titanite is of igneous origin. Allanite and zircon inclusions that produce pleochroic halos in the hornblende are also identified. The oxide analysis reveals a SiO_2 proportion of 56.12% that indicates a dioritic composition, supported by the presence of a normative quartz proportion of 7.8%. As regards the plagioclase, its normative composition ($Ab_{53}An_{47}$) coincides with its optical identification as andesine. The protolith of these rocks is interpreted as a diorite to monzodiorite because of the presence of variable amounts of K feldspar (7.7% normative orthoclase).

4.2.2. Metagranite

This rock has a grayish pink color and is medium grained. Its metamorphic character is only evidenced by the deformation: i.e. elongated and oriented components due to pressure; they encompass quartz, K-feldspar, plagioclase (sodic andesine), muscovite and garnet. Quartz is present as slightly fractured grains, with marked wavy extinction and scarce aligned fluid inclusions. K-feldspar has scarce perthites and is slightly altered to clays; it locally tends to develop higher grain size in respect to the other minerals. Andesine shows sometimes curved albite-Carlsbad twinning, some minor clay alteration and replacement by K-feldspar following the twinning planes. Muscovite appears as very scarce short flakes. Garnet (Alm_{70}-Sps_{30}) forms euhedral to subhedral crystals (up to 2 mm), usually of poikilitic character due to K-feldspar inclusions, and it is fractured due to the overall deformation (Fig. 3e).

5. Geochemistry

Chemical analyses of the main lithologic types of the El Carancho Igneous Complex are given in Table 1 (see Supplementary Data). Unaltered and homogeneous samples were selected for chemical analyses, and performed at Activation Laboratories Ltd. of Canada. Techniques and procedures can be found at www.actlabs.com. Whole rock chemical analyses in an AFM diagram (Fig. 4a) show that the El Carancho Igneous Complex includes two meta-magmatic suites. The metadiorites and metagranites belong to the calc–alkaline field coinciding to the Pampean magmatic arc field defined to the north (cf. Lira et al., 1997). The second trend includes metagabbros and metapyroxenites that correspond to a tholeiitic suite.

In order to distinguish and discriminate the tectonic setting for both suites several discrimination diagrams were used considering elements whose signatures and ratios are determined by igneous petrogenesis and are not affected by post-magmatic mobilization.

Following the petrographic observation we can assume that the metamorphism did not change the overall chemistry of the Complex. Under this premise its normative composition reflects the original composition of the magmatic protoliths, i.e. dioritic–granitic and gabbroic–pyroxenitic (Two samples – 131BF and BF2 – show high silica content – 70.61 and 71.08% – because of secondary quartz injected during metamorphism, and they are not considered for this purpose) (Table 1, see Supplementary Data).

The Ti–Zr diagram (Pearce and Cann, 1973) can be used to distinguish ocean floor and volcanic arc mafic rocks. Samples from the tholeiitic suite fall in the MORB field whereas the metadiorite from the calc–alkaline suite plots in the volcanic arc basalt field (Fig. 4b).

5.1. Tholeiitic suite

The metagabbros and metapyroxenites have an E-MORB geochemical signature with SiO_2 ranging between 48.35 and 52.08%. The normative composition of plagioclase from the metapyroxenites corresponds to calcic bytownite–anorthite; metagabbros have normative labradorite. All samples are classified as subalkaline in the ($Na_2O + K_2O$) versus SiO_2 diagram (Irvine and Baragar, 1971). The spider diagram (Fig. 4c) shows that the LIL elements, that are more mobile, vary as a result of the effect caused by the metamorphism, whereas the less mobile HFS elements exhibit a flat profile. Small Ta and Nb negative anomalies suggest a minor contamination with crustal components. The Nb/Th ratio varies from 2.7 to 11.25.

LREE (Fig. 4d) are slightly enriched, with chondrite normalized $(La/Yb)_N$ values between 1.68 and 5.34, (Sm/La) between 0.45 and 0.85, (La/Yb) between 1.68 and 5.34, and (Gd/Yb) between 1.16 and 2.00. Values point to a restricted degree of REE fractionation.

In the Zr/4-Nb*2-Y discriminant diagram (Meschede, 1986) metagabbros and metapyroxenites are also grouped in the MORB field (Fig. 4e).

The Cr–Y discrimination diagram (after Pearce, 1982; Fig. 4f) shows that the mafic rocks of the tholeiitic suite are derived from a mantle source that underwent 5–20% partial melting followed by fractionation.

5.2. Calc–alkaline suite

All analyzed rocks of the suite plot in the subalkaline field in the $Na_2O + K_2O$ versus SiO_2 diagram (Irvine and Baragar, 1971). In the AFM diagram (Fig. 4a) they show a calc–alkaline fractionation trend that starts with diorites and ends, after a gap, with granites, being grouped into two separate fields already identified in the Pampean magmatic arc rocks from Sierra Norte–Sierra de Ambargasta (Lira et al., 1997). Zr/Y ratios, varying from 1.59 to 12.68, indicate a calc–alkaline fractionation trend. The metagranites plot in the syncollisional granites field of the Rb versus Y + Nb discriminant diagram (Pearce et al., 1984).

The chemical analysis of garnet from the metagranite (performed using an EDX coupled scanning electron microscope) yielded almandine–spessartite ($Alm_{67.6-72.6}Sps_{32.4-27.3}$). Its late crystallization may result from the increase of the Mn/(Mn + Fe) ratio during the evolution of the suite (cf. Miller and Stoddard, 1980). The presence of manganese increases the field of garnet stability allowing its crystallization under very low pressures; spessartite-rich garnets can crystallize in equilibrium with a granitic melt under pressures of ca. 3 kbar or less (Green, 1977).

MORB normalized multielement pattern (Fig. 4g) shows an enrichment in LIL elements (K_2O, Rb, Ba) and a depletion of HFS elements (Ce, P_2O_5, Zr, Hf, Sm, Ti), that is characteristic from melts formed in an active continental margin setting, although the mobility of LIL elements by metamorphism is not excluded.

The chondrite normalized $(La/Yb)_N$ value of 3.46 for the metadiorite is indicative of a LREE enrichment. Metagranites show a slight depletion of light REE (LREE) and Eu, and a clear enrichment of heavy REE (HREE) with $(La/Yb)_N$ values up to 0.44. This evolution leads to HREE-enriched leucogranites with "wing-shaped" distribution patterns (Fig. 4h) in chondrite-normalized diagrams. The latter pattern may result from garnet fractionation.

6. Geochronological data

6.1. U–Pb SHRIMP dating

6.1.1. Methodology

Samples MG91b (metadiorite) and MG91c (metapyroxenite) were collected in the proximity of the El Carancho estate (see Fig. 1). The rocks were crushed, milled, sieved at 60 Mesh, and washed to remove the clay and silt fractions. The remaining material, corresponding to fine sand and very fine sand, was dried and processed by two heavy liquids: LST (lithium–sodium tungstate, density 2.8) and TBE (tetrabromo-ethane, density 3). The heavy mineral concentrates were separated into four fractions using a Frantz® magnetic separator. Zircon and titanite grains were picked from the less magnetic fraction at 1 A and 5° inclination and then mounted in an epoxy disk of 2.5 cm diameter together with the analytical standards. The mount was polished and coated with carbon for imaging using a JEOL6400 Scanning Electron Microscope at the Centre for Microscopy, Characterization and Microanalyses of the University of Western Australia. This carbon coating was removed and replaced for a gold coating for SHRIMP U–Pb analyses.

Table 2
Isotopic data (U–Pb and Hf) of zircons of metadiorite (sample MG91b).

Spot	U	Th	Th	Pb	4f206	Isotopic ratios					Ages		Disc. %	Hf	
						^{207}Pb	^{208}Pb	^{206}Pb	^{207}Pb	^{208}Pb	^{207}Pb	^{206}Pb		model-age	ε
	ppm	ppm	U	ppm	(%)	^{206}Pb	^{206}Pb	^{238}U	^{235}U	^{232}Th	^{206}Pb	^{238}U		Ma	
d.1-1	400	2	0.005	28.5	0.05	0.05751 ± 1.59	0.0019 ± 7.27	0.0829 ± 0.88	0.6572 ± 1.81	–	511 ± 35	513 ± 4	−0.4	850	9.77
d.1-2	115	52	0.467	20.1	0.19	0.07987 ± 1.38	0.1347 ± 1.15	0.2033 ± 0.96	2.2389 ± 1.68	0.057 ± 2.3	1194 ± 27	1193 ± 10	0.1	1624	5.77
d.1-2b														1720	4.28
d.1-3	69	44	0.66	11.7	0.12	0.07773 ± 1.85	0.1941 ± 1.16	0.1988 ± 1.11	2.1306 ± 2.16	0.0577 ± 2.1	1140 ± 37	1169 ± 12	−2.5	1684	4.12
d.2-1	579	7	0.013	40.9	0.17	0.05764 ± 1.02	0.0045 ± 3.44	0.082 ± 0.86	0.6518 ± 1.33	–	516 ± 22	508 ± 4	1.5	810	10.3
d.3-1	662	3	0.005	47.6	0.06	0.05762 ± 1	0.0019 ± 5.72	0.0836 ± 0.85	0.6638 ± 1.31	–	515 ± 22	517 ± 4	−0.4	895	9.04
d.3-2	364	3	0.007	26.7	0.1	0.05762 ± 1.25	0.0032 ± 5.86	0.0853 ± 0.89	0.6778 ± 1.54	–	515 ± 28	528 ± 4	−2.4		
d.4-1	574	4	0.007	41.6	0.01	0.05695 ± 0.97	0.0026 ± 5.22	0.0843 ± 0.83	0.6623 ± 1.27	0.0311 ± 18.79	490 ± 21	522 ± 4	−6.6		
d.5-1	398	4	0.01	28.9	0.02	0.05831 ± 0.96	0.004 ± 4.88	0.0847 ± 0.88	0.6806 ± 1.3	0.0315 ± 11.1	541 ± 21	524 ± 4	3.2		
d.6-1	530	4	0.007	38.8	0.01	0.05793 ± 0.93	0.0024 ± 5.87	0.0852 ± 0.86	0.6805 ± 1.27	0.0254 ± 28.9	527 ± 20	527 ± 4	0	876	9.49
d.6-2	494	3	0.006	35.8	0.08	0.05762 ± 1.13	0.0024 ± 6.06	0.0843 ± 0.87	0.67 ± 1.42	–	515 ± 25	522 ± 4	−1.2	990	7.58
d.7-1	613	4	0.007	44.3	0.04	0.05575 ± 0.78	0.0023 ± 5.46	0.0842 ± 0.82	0.6704 ± 1.13	0.0165 ± 18.58	521 ± 17	521 ± 4	−0.1		
D.8-1	506	3	0.007	36.3	0.09	0.05805 ± 0.99	0.0026 ± 5.39	0.0835 ± 0.86	0.6683 ± 1.31	–	532 ± 22	517 ± 4	2.8		

Sensitive High Mass Resolution Ion MicroProbe (SHRIMP II) U–Pb analyses were performed at Curtin University of Technology in two sessions using an analytical spot size of about 20–25 μm. Individual analyses are composed of nine measurements repeated in five scans. The following masses were analyzed for zircon: (Zr_2O, ^{204}Pb, background, ^{206}Pb, ^{207}Pb, ^{208}Pb, ^{238}U, ^{248}ThO, ^{254}UO), and ($^{200}CaTi_2O_4$, ^{204}Pb, background, ^{206}Pb, ^{207}Pb, ^{208}Pb, ^{248}ThO, ^{254}UO, $^{270}UO_2$), for titanite. The standards D23 and NBS611 were used to identify the position of the peak of the mass ^{204}Pb, whereas the calibration of the U content and the Pb/U ratio were done using the zircon standard BR266 (559 Ma, 903 ppm U). For titanite the standard used for calibration is Khan (522 Ma; 510 ppm U). Data were reduced using the SQUID© 1.03 software (Ludwig, 2001) and the ages calculated using Isoplot© 3.0 (Ludwig, 2003). The presented Cambrian age is mean average $^{206}Pb/^{238}U$ age whereas the Mesoproterozoic ages are mean average $^{207}Pb/^{206}Pb$ ages all calculated at 2σ level. The individual analyses are quoted at 1σ level (Table 2).

6.1.2. Results

6.1.2.1. Sample MG91b (metadiorite). The zircon population has two grains with Mesoproterozoic cores dated at 1193 ± 10 Ma and 1140 ± 37 Ma (spots d.1-2 and d.1-3)(Fig. 5a). These cores have magmatic origin showing zoning and relatively high Th/U ratios (0.467 and 0.660). The rims and other 10 dated zircons (Table 2) have the same $^{206}Pb/^{238}U$ age pooled at 520 ± 1.4 Ma (MSWD = 0.013; probability = 0.91)(Fig. 5b). The older cores have less U (average is 92 ppm) whereas the Cambrian zircons have more U (average is 512 ppm). The Cambrian ages are from zoned rims (d.1-1), unzoned rims (grains d.4-1, d.6-1, d.6-2, d.7-1) and from zoned cores (d.3-1, d.3-2) having characteristics of metamorphic (unzoned) and magmatic (zoned) zircon. All Cambrian zircons have very low Th content (average is only 4 ppm) and consequently very low Th/U ratios (average = 0.07) which are characteristics of metamorphic zircon. Some of the Cambrian zircons still preserve magmatic zoning and this may be related to the fact that metamorphism did not reach granulite conditions. The syncollisional nature of the dated metadiorite permits to interpret that the Cambrian age of 520 ± 1.4 Ma of crystallization is not distinguishable with the timing of the metamorphic event considering that the time difference between magmatism and metamorphism could be less than 1 m.y.

6.1.2.2. Sample MG91c (metapyroxenite). Sample MG91c has magmatic titanite, which is dark reddish brown occurring as shards of 500–600 μm in diameter. The mineral is U-poor (average is 21 ppm) and a larger analytical spot of about 40 μm was used to compensate the low U content. The results (Table 3) are concordant to subconcordant but subjected to a strong common lead correction (using the ^{204}Pb values). Analysis has a common lead correction of 455 and this result is not used in the age calculation. The mean average of the $^{206}Pb/^{238}U$ ages is 528 ± 7 Ma but with a MSWD of 4.3. The concordia age of seven analyses (excluding grains d.1-1 with high common lead correction and d.1-4, 40% discordant) is 528 ± 5 Ma (MSWD = 0.019)(Fig. 6) and this is the best estimate for the emplacement of the pyroxenite. This titanite is Th-rich having large Th/U ratios of up to 5.48 (average is 2.74). The average Th/U ratio of the modern upper mantle is 2.6 (bulk earth = 4) and the high values present in MG91c indicate that the magma which generated the rock has a strong mantle input, being a juvenile magmatism. The Th/U ratio of the mantle at the time of the El Carancho magmatism (528 Ma) was around 3.2 (considering the model of Elliot et al., 1999) or 2.8 according to Allègre et al. (1986) or 2.6 following Galer and O'Nions, 1985. All these values are comparable to the Th/U ratio of the titanites of El Carancho pyroxenite which may have been directly extracted from the upper mantle.

The relatively large amount of common lead in titanite (when compared to other minerals such as zircon) is a common feature of

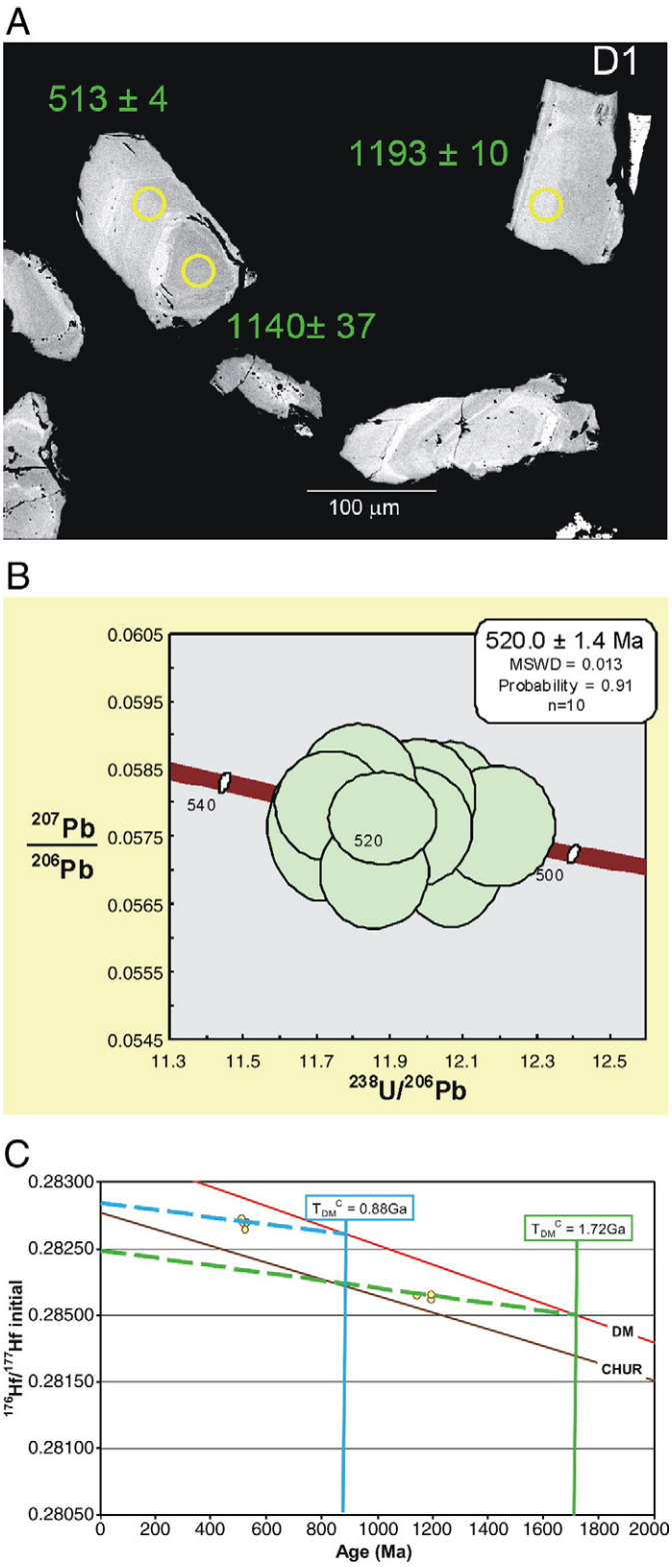

Fig. 5. a): Back-scattered electrons image of some zircons of sample MG91b (metadiorite) showing older magmatic Mesoproterozoic cores (1193 and 1140 Ma) and Cambrian magmatic rim (513 Ma). b): Inverse concordia plot of magmatic zircon ages of metadiorite. The concordia age at 1 sigma is 520 ± 1.4 Ma. Ages of inherited Mesoproterozoic zircon (1193 Ma and 1140 Ma) not shown. c): Plot of $^{176}Hf/^{177}Hf$ ratios versus ages of eight dated zircons of sample MG91b (metadiorite). The Depleted Mantle model-age (crustal) is Early Neoproterozoic (884 Ma). The slope of the dashed line uses the ratio of 0.015 for the $^{176}Lu/^{177}Hf$ ratio.

Table 3
U–Pb titanite SHRIMP isotopic data of metapyroxenite (sample MG91c).

Spot	U	Th	Th	Pb	4f206	Isotopic ratios					Ages		Disc.
						$^{207}Pb/^{206}Pb$	$^{208}Pb/^{206}Pb$	$^{206}Pb/^{238}U$	$^{207}Pb/^{235}U$	$^{208}Pb/^{232}Th$	$^{207}Pb/^{206}Pb$	$^{206}Pb/^{238}U$	%
	ppm	ppm	U	ppm	(%)								
D.1-4	21	18	0.93	1.83	15.67	0.05437 ± 65.9	0.8939 ± 2.30	0.0875 ± 4.72	0.6558 ± 66.0	0.0629 ± 14.8	386 ± 1479	541 ± 24	−40
D.1-5	21	22	1.08	1.94	20.60	0.05656 ± 32.2	1.0530 ± 1.93	0.0864 ± 2.47	0.6740 ± 32.3	0.0623 ± 8.5	474 ± 712	534 ± 13	−13
D.1-6	10	22	2.25	0.77	5.64	0.05817 ± 12.0	0.1237 ± 3.38	0.0849 ± 1.50	0.6811 ± 12.1	–	536 ± 262	525 ± 8	2
D.1-7	8	43	5.48	0.62	3.51	0.05747 ± 6.4	0.0764 ± 1.81	0.0862 ± 1.18	0.6831 ± 6.51	–	510 ± 141	533 ± 6	−5
D.1-8	84	88	1.08	8.06	21.17	0.06664 ± 27.9	0.7365 ± 1.38	0.0883 ± 2.63	0.8115 ± 28.0	0.0300 ± 18.3	827 ± 581	546 ± 14	34
D.1-9	19	41	2.19	1.40	1.98	0.05739 ± 4.6	0.0543 ± 1.88	0.0835 ± 1.10	0.6651 ± 4.64	0.0005 ± 58.1	520 ± 99	517 ± 5	1
D.2-1	9	22	2.52	0.69	2.82	0.05821 ± 13.7	0.0716 ± 3.90	0.0868 ± 2.11	0.6970 ± 13.9	–	537 ± 301	537 ± 11	0
D.3-1	10	46	4.59	0.78	2.43	0.05891 ± 7.6	0.0518 ± 3.80	0.0856 ± 1.78	0.6951 ± 7.85	–	564 ± 166	529 ± 9	6

this mineral (Frost et al., 2000). Sample MG91c has common Pb ranging from 0.02 to 1.7 ppm and U from 8 to 84 ppm (Table 3); the initial U/common Pb ratio ranges from 53.3 to 686.35. These data are in agreement with Frost et al. (2000), for whom titanite from igneous rocks has initial U contents ranging from 10 to over 100 ppm and ratios of initial U to common Pb ranging from 10 to 1000. The magmatic nature of the titanite from sample MG91c is also consistent with its euhedral boundaries and planar contact with other magmatic phases (Fig. 3b), contrary to metamorphic titanite, which usually occurs as subhedral to anhedral fine grained disseminated crystals within chlorite (after chloritization of biotite), or as rims around ilmenite, or as coarse lenticular grains with inclusions of ilmenite and surrounded by albitic plagioclase (formed by titanization of ilmenite by a reaction with Ca-plagioclase bellow 750 °C), or aligned, parallel to needles of biotite and hornblende, if associated with shearing (*c.f.* Essex and Gromet, 2000; Mohammad and Maekawa, 2008; Raimondo et al., 2009).

6.2. Hf isotopes

6.2.1. Methodology

Hf-isotope analyses were carried out using a New Wave/Merchantek UP213 laser-ablation microprobe, attached to a Nu Plasma multi-collector ICP-MS at GEMOC (Geochemical Evolution and Metallogeny of Continents), Macquarie University, Sydney. Operating conditions include a beam diameter of ~55 μm, a 5 Hz repetition rate, with energy of ~0.4–0.8 mJ. Typical ablation times were 100–120 s, resulting in pits 40–60 μm deep. Mud Tank (MT) zircon was used as reference material which has an average $^{176}Lu/^{177}Hf$ ratio of 0.282522 ± 42 (2SE) (Griffin et al., 2007). MT analyzed in this study was within reported range (0.282514 ± 26; n = 2). More detail of the analytical techniques, precision and accuracy is described by Griffin et al. (2000, 2004).

Initial $^{176}Hf/^{177}Hf$ ratios are calculated using measured $^{176}Lu/^{177}Hf$ ratios, with a typical 2 standard error uncertainty on a single analysis of $^{176}Lu/^{177}Hf$ ± 1–2%. Such error reflects both analytical uncertainties and intragrain variation of Lu/Hf typically observed in zircons. Chondritic values of Scherer et al. (2001) (1.865×10^{-11}) have been used for the calculation of ε_{Hf} values. While a model of $(^{176}Hf/^{177}Hf)_i = 0.279718$ at 4.56 Ga and $^{176}Lu/^{177}Hf = 0.0384$ has been used to calculate model ages (T_{DM}) based on a depleted-mantle source, producing a present-day value of $^{176}Hf/^{177}Hf$ (0.28325) (Griffin et al., 2000, 2004). T_{DM} ages, which are calculated using measured $^{176}Hf/^{177}Hf$ of the zircon, give only the minimum age for the source material from which the zircon crystallized. We have therefore also calculated a "crustal" model age (T^C_{DM}) for each zircon which assumes that the parental magma was produced from an average continental crust ($^{176}Lu/^{177}Hf = 0.015$) that was originally derived from depleted mantle.

6.2.2. Results

Eight measurements for Hf isotopes were undertaken on seven zircon crystals of sample MG91b (metadiorite). The $^{176}Hf/^{177}Hf$ ratios range 0.282161 to 0.282736 and all grains have positive ε_{Hf} (from 4.11 to 10.29) and plot above the depleted mantle model line using the Blichert-Toft and Albarède (1997) ^{176}Lu decay constant of 1.93×10^{-11} (Table 2 and Fig. 5c).

Average Hf T_{DM} of Cambrian zircons is 884 Ma and the ε_{Hf} values are all high (average = +9.24) indicating that the melt which formed the diorite has strong juvenile input. The Mesoproterozoic inherited zircons also have Hf characteristics of juvenile source: T_{DM} average age of 1674 Ma and ε value (average) of +4.72.

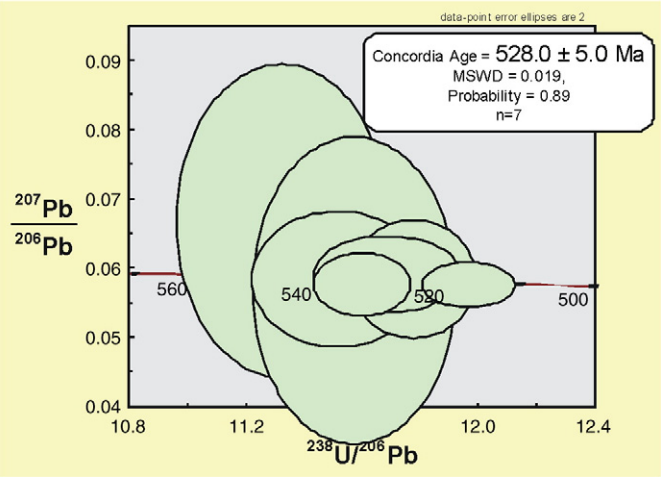

Fig. 6. Inverse concordia plot of titanite of sample MG91c (metapyroxenite) providing a concordant age of 528 ± 5 Ma (2 sigma; n = 7).

7. Discussion

7.1. Juvenile segment of the Pampean magmatic arc and the basement of southern Pampia terrane

The juvenile character of the poorly exposed segment of the Pampean (ca. 520 Ma) magmatic arc at the province of La Pampa (El Carancho Igneous Complex) is inferred from the Hf isotope composition of the Cambrian zircons of the calc–alkaline metadiorites of the Complex. Their $\varepsilon_{Hf(520\ Ma)}$ values range +7.58 to +10.29, and their Hf model ages yield 884 Ma (Early Neoproterozoic). This would mean that the metadiorites crystallized from an Early Neoproterozoic (Tonian) juvenile source that could well represent an extensional episode of magmatism pertaining to the early stage of the Rodinia breakup, developed within the mostly Paleo-Mesoproterozoic basement of Pampia (Chernicoff et al., 2011a,b).

It may be possible that the Late Neoproterozoic (Brasiliano-age; Sm–Nd isochron ca 647 Ma) oceanic backarc envisaged to occur in the Eastern Sierras Pampeanas of Córdoba (Escayola et al., 2007) could also derive from the same juvenile Tonian source, given the

Table 4
U–Pb SHRIMP and Hf isotope determinations from Lower Paleozoic magmatic units, and from Neoproterozoic–Lower Paleozoic metasedimentary units, La Pampa province.

Zircon type	Unit	Rock type	Tectonic setting	U–Pb SHRIMP age	Epsilon Hf	TDM (Hf)	Source of data
Magmatic	Paso del Bote Formation	Metaquartz-diorite, metagabbro, etc.	Famatinian arc	476–466 Ma	−5 to −3.6	Average 1720 Ma	Chernicoff et al., 2010a
Magmatic	Valle Daza Formation	metagabbro	Famatinian backarc	ca. 450 Ma	All positive values, +7 to +10.	Average 880 Ma	Chernicoff et al. (2008c, 2009, 2011a,b)
Magmatic	El Carancho Igneous Complex	metadiorite	Pampean arc	ca. 520 Ma	All positive values, +7.18 to +9.37	ca. 884 Ma	This paper
Magmatic	El Carancho Igneous Complex	metapyroxenite	Pampean backarc	ca. 528 Ma	No data	No data	This paper
Detrital	Santa Helena Schist	metasediments	Foreland basin associated with Pampean orogeny	Age range of deposition ca. 556 to ca. 520 Ma	Dominantly positive values, (mostly) +2 to +11	Mostly ca. 1200 to ca. 1900 Ma	Zappettini et al. (2010)
Detrital	Green Schist	metasediments	Post-collisional basin, associated with Pampean orogeny	Age range of deposition ca. 500–515 to ca. 465 Ma	Equal number of positive and negative values, (mostly) −5 to +11	Mostly ca. 1200 to ca. 1800 Ma	Chernicoff et al. (2007, 2008b); this paper
Detrital	La Horqueta Formation	metasediments	Foreland basin associated with Famatinian orogeny	Age range of deposition ca. 466 to 405 Ma	90% negative values: (mostly) −2 to −8	90% in the range 1400 to 1950 Ma	Chernicoff et al. (2008d)

positive ε_{Nd} value of 5.2 yielded by its constituting ophiolite remnants, and the single (continuous) Brasiliano–Pampean magmatic process (see below).

Juvenile Tonian magmatic rocks must have been exposed in La Pampa province in Late Neoproterozoic–Early Cambrian times (Chernicoff et al., 2011a,b), as evidenced by the detrital zircon population of this age and character (999–871 Ma; ε_{Hf} +2.69 to +7.39) identified in the Santa Helena Schist (Zappettini et al., 2010); the latter metasedimentary rocks are regarded to pertain to the late Puncoviscana basin (i.e., Puncoviscana Formation proper, and higher-grade correlative metasedimentary rocks in the Eastern Sierras Pampeanas). Previous data (e.g. Escayola et al., 2007, and references therein; Adams et al., 2008, and references therein) also identified Tonian detrital zircon grains in the Puncoviscana metasedimentary rocks.

In addition, the studied segment of the Pampean magmatic arc is contaminated by also juvenile, Late Mesoproterozoic crust (1140–1194 Ma; ε_{Hf} +4.12 to +5.77; T_{DM}-Hf 1674 Ma) as evidenced by the presence of xenocrystic cores in the dated zircons. We argue that these data indicate that the juvenile Pampean magmatic arc was intruded into juvenile Late Mesoproterozoic magmatic arc rocks, reinforcing previous data (Zappettini et al., 2010; and Hf isotope data for the Green Schist, see Table 4) that suggest that magmatic rocks possibly belonging to a juvenile Mesoproterozoic arc underlie this region. It should be noticed that the latter previous data suggested the occurrence of a juvenile magmatic arc at around 1400 Ma, comparable with the juvenile Santa Helena arc of the Sunsás orogen (Santos et al., 2008), whereas our present data may indicate the occurrence of another, slightly younger, juvenile arc at ca. 1100 Ma that may be equivalent to the mafic rocks associated to the late orogeny within the Sunsás Orogen, the Nova Brasilândia orogeny (Rizzotto et al., 1999) of Brazil–Bolívia region. Recent study combining LA-MC-ICP-MS U–Pb dating and Hf isotope determinations on latest Ediacaran to Ordovician metaturbidites of NW Argentina, has identified juvenile (ε_{Hf} ca. +5 to ca. +10) Mesoproterozoic zircon grains that encompass the whole range from ca. 1100 Ma to ca. 1400 Ma (cf. Fig. 2, Hauser et al., 2010a, 2010b).

However, we are not implying that the Mesoproterozoic basement of southern Pampia is solely composed of juvenile magmatic arc rocks, since we have also collected evidence for the existence of a reworked Paleo-Mesoproterozoic component in this basement; Table 4 summarizes our data on Hf isotope determinations on both detrital and magmatic zircons from Neoproterozoic–Lower Paleozoic cover sequences and from Lower Paleozoic magmatic units, respectively. This summary denotes that the proportions – and unknown geographic distribution – of the reworked Paleo-Mesoproterozoic and juvenile Mesoproterozoic components – plus a more limited component of juvenile Lower Neoproterozoic (Tonian) crust – can still not be fully assessed. In any case, we consider that the mostly Paleo-Mesoproterozoic basement of southern Pampia would represent continental crust, and constitute the actual substratum of the Puncoviscana basin (at the latitude of La Pampa province, represented by the Santa Helena Schist).

It is worth noting that a coeval, unexposed Proterozoic basement is also regarded to have been the source of the Paleozoic magmatic rocks intruded in the Patagonia terrane of southern Argentina–Chile (e.g. Augustsson et al., 2006; Pankhurst et al., 2006), regardless of whether or not this basement ever formed part of a single tectono-stratigraphic unit (a largely Mesoproterozoic orogen) with the basement of La Pampa region (and that of central-northern Argentina). A close inspection of the Nd model ages and ε_{Nd} values of the granitoids and Lower Paleozoic metasedimentary rocks of the North Patagonian Massif-NPM (e.g. Pankhurst et al., 2006, and references therein) reveals that this basement block would be predominantly underlain by reworked Paleo-Mesoproterozoic crust and a minor, juvenile Early Neoproterozoic (Tonian) crust, much like the southern Pampia

Table 5
Rim and core magmatic and detrital zircon ages from the El Carancho Igneous Complex (this paper), and from the Cambrian Green Schist, Negro Peinado Formation and Achavil Formation. Ages given in Ma. (1): spot D.1-1 has T_{DM}-Hf 888 Ma and εHf +9.37; (2): spot D.1-3 has T_{DM}-Hf 1768 Ma and εHf +3.24.

Unit	Spot	Rim	Core	Reference
Green Schist (sample MG29)	2-10/2-9	508	1923	Chernicoff et al. (2008b) and new data for sample MG29 (this paper)
El Carancho Igneous Complex (sample MG91b)	D.1-1/D.1-3	513 (1)	1140 (2)	This paper
Negro Peinado F.	07/08	516	1033	Collo et al. (2009)
Negro Peinado F.	29/28	536	1689	Collo et al. (2009)
Green Schist (sample MG29)	a.7-6/a.7-7	539	1022	Chernicoff et al. (2008b) and new data for sample MG29 (this paper)
Negro Peinado F.	63/64	562	997	Collo et al. (2009)
Achavil F.	50/51	614	2045	Collo et al. (2009)
Negro Peinado F.	33/32	633	1016	Collo et al. (2009)

basement (a juvenile Mesoproterozoic component may eventually be detected in the NPM by Hf isotope determinations on SHRIMP dated zircons). In southwestern Patagonia, the source material of the magma from which most zircon grains crystallized is either juvenile or reworked Paleo-Mesoproterozoic crust (neither of the two components dominate), and minor juvenile Early Neoproterozoic (Tonian) crust, as detected by Hf isotope studies of single detrital zircons of Late Paleozoic metasediments (Augustsson et al., 2006).

As regards the juvenile nature of the studied segment of the Pampean magmatic arc, this differs from the derivation of the main outcrops of the arc exposed in the Sierras Pampeanas of Córdoba province, where the negative epsilon Neodimium values of the Cambrian igneous rocks point to a reworked crustal origin (e.g. Rapela et al., 1998). However, since it has been demonstrated that I-type magmatism critically involves continental growth (juvenile additions) that can be camouflaged to some extent by the non-mantle-like isotope ratios of the bulk rocks (Kemp et al., 2007), a juvenile component may still be expected to occur in the main exposures of the Pampean arc.

Elsewhere, evidence of juvenile Cambrian magmatism has been found e.g. in a segment of the Ross orogen (Robertson Bay terrane, Victoria Land), inferred to be underlain by a thinned crust of Tonian age (Nd model ages averaging 980 Ma, and positive epsilon Nd values; Gemelli et al., 2009; Rocchi et al., 2010). Similarly, the inferred presence of juvenile Tonian magmatic rocks in the (otherwise, mostly Paleo-Mesoproterozoic) substratum of southern Pampia could indicate a zone of thinned basement, possibly associated with the early stage of Rodinia's breakup.

7.2. A single Brasiliano–Pampean magmatic arc

An implication of the model preferred herein for the Pampean orogen (see also Geological Framework, above), that involves i) detachment of a 'ribbon' (Pampia terrane) of the Río de la Plata craton's outer belt (largely Mesoproterozoic orogen) from its Paleoproterozoic–Archean nucleus, prior to 600 Ma, concomitant with ii) formation of a basin within this detached fragment (Puncoviscana basin), iii) west dipping subduction of oceanic crust beneath the Pampia terrane starting possibly by ca 585 Ma (e.g. Schwartz et al., 2008) and iv) reaccretion of the Pampia terrane to the Río de la Plata craton at 530–520 Ma, is the uninterrupted development of arc magmatism on the Pampia terrane (upper plate) from Brasiliano to Pampean times. Schwartz et al. (2008) also suggested uninterrupted development of arc magmatism but due to subduction toward the east beneath the Río de la Plata craton, contrary to our model of west dipping subduction beneath the Pampia terrane. Our scheme also differs from that proposed by Collo et al. (2009) who favor two separate unrelated subduction processes, with opposite polarity, i.e. firstly west dipping subduction beneath the Pampia terrane (considered as southern extension of Arequipa–Antofalla) would have generated a Brasiliano magmatic arc and accretion of the Pampia terrane to the Río de la Plata craton, prior to opening of the Puncoviscana basin within the Pampia terrane, and secondly, closing of the Puncoviscana basin through east dipping subduction beneath the Pampia terrane would have generated the Pampean magmatic arc (Brasiliano and Pampean arcs, respectively located east and west of Puncoviscana rifting).

Evidence for the uninterrupted development of arc magmatism on the Pampia terrane (upper plate) from Brasiliano to Pampean times, as proposed in our model, is given by the occurrence of numerous examples of zircons (either detrital or magmatic) that record Brasiliano age to Cambrian rims, and Paleoproterozoic to late Mesoproterozoic cores, as summarized in Table 5: the rim ages would indicate a relatively continuous magmatism recorded at 633 Ma, 614 Ma, 562 Ma, 539 Ma, 536 Ma, 516 Ma, 513 Ma and 508 Ma, intruded into Paleoproterozoic–Mesoproterozoic host rocks (represented by the zircon cores).

It should be noted that of all the long lasting subduction process – started in the Late Neoproterozoic – , the late Early Cambrian stage must have involved a concomitant extension, as suggested by the occurrence of E-MORB-type metapyroxenites and metagabbros in the El Carancho Igneous Complex, herein interpreted as relics of oceanic mantle-derived rocks emplaced in the back-arc of the active margin. In this scenario, the minor meta-analcime gabbros (metateschenites) may represent the incipient stage of this extension.

7.3. Post-Pampean to Upper Paleozoic events in the southern Pampia terrane

The occurrence of post-collisional metasediments in southern Pampia is represented by the Green Schist, deposited between 500–515 Ma and 465 Ma in a post-collisional basin mostly sourced from the Pampean orogen (Chernicoff et al., 2007, 2008b; Zappettini et al., 2010). Further north, in the Famatina ranges of central Argentina, roughly coeval metasediments have been interpreted as syn-collisional (Negro Peinado and Achavil Formations; Collo et al., 2009).

Following the termination of the Pampean orogeny, and after a period of quiescence during the Late Cambrian (e.g. Rapela et al., 1998), an east-dipping subduction zone was established at the western margin of Pampia–Gondwana. This new (Famatinian) subduction led to the collision of the Cuyania terrane in the Middle to Late Ordovician (465–450 Ma, as established in La Pampa; Chernicoff et al., 2008a, 2009), causing the deformation of the protolith of the Green Schist.

In the province of La Pampa it has been identified the southernmost segment of the Famatinian magmatic arc, mainly represented by metaquartz-diorites and metagabbros (Paso del Bote Formation) dated at ca. 466–476 Ma (Chernicoff et al., 2010a). A belt of MORB-type metagabbros dated at ca 450 Ma (Valle Daza Formation) and attributed to pertain to the Famatinian magmatic back-arc (Chernicoff et al., 2008c, 2009) has also been identified in the region.

A depocenter of a Late Ordovician–Devonian marine foreland basin generated after Cuyania's accretion (Curacó Basin) lies immediately west of the Pampia terrane (Gondwana)/Cuyania boundary, it being filled by sandstones and shales of the La Horqueta Formation, that represents the southern continuation of the same unit exposed in the San Rafael Block (Chernicoff et al., 2008d).

Gondwanan (Permo-Triassic) magmatism straddles the boundaries of all the tectono-stratigraphic terranes in the study region, reaching also the Río de la Plata craton. It comprises intermediate to acidic volcanic and pyroclastic rocks, leucogranites and syenites of the Lihuel Calel Group (Espejo and Silva Nieto, 1996). The latter rock type has recently been dated at 243 ± 8 Ma (K–Ar on amphibole, Lagorio et al., 2008). Also, there is evidence of Permian mylonitization of the Silurian granitoids (e.g. at Cerro de los Viejos; deformation dated at ca. 261 Ma; K–Ar in muscovite, Tickyj et al., 1997), that roughly follows the Rio de la Plata craton (WNW trending) basement fabric. The latter deformation pertains to the Gondwanide event, more conspicuously represented in the Sierra de la Ventana fold and thrust belt (i.e. synorogenic deformation of the Las Tunas Formation, e.g. López Gamundi et al., 1995), located about 200 km to the east of the present study area.

Fig. 7 presents a schematic model for the Pampean orogen at the latitude of La Pampa province, within the broader context of the tectonic evolution of the southwestern Gondwana margin up to Ordovician times (Fig. 7g); the starting point is the proposed Mesoproterozoic orogen (Fig. 7a; possible southern continuation of the Sunsás belt of SW Amazonas) located at the western border of the Río de la Plata craton (see also Fig. 17, in Gaucher et al., 2008, and Fig. 6, in Aceñolaza and Toselli, 2009). The MORB-type metapyroxenites and metagabbros of the El Carancho Igneous Complex are herein regarded to correspond to oceanic mantle-derived rocks emplaced in the backarc (not drawn in Fig. 7e, for the sake of clarity), and tectonically imbricated with the arc-type metadiorites and metagranites of the Complex during the Pampean collision.

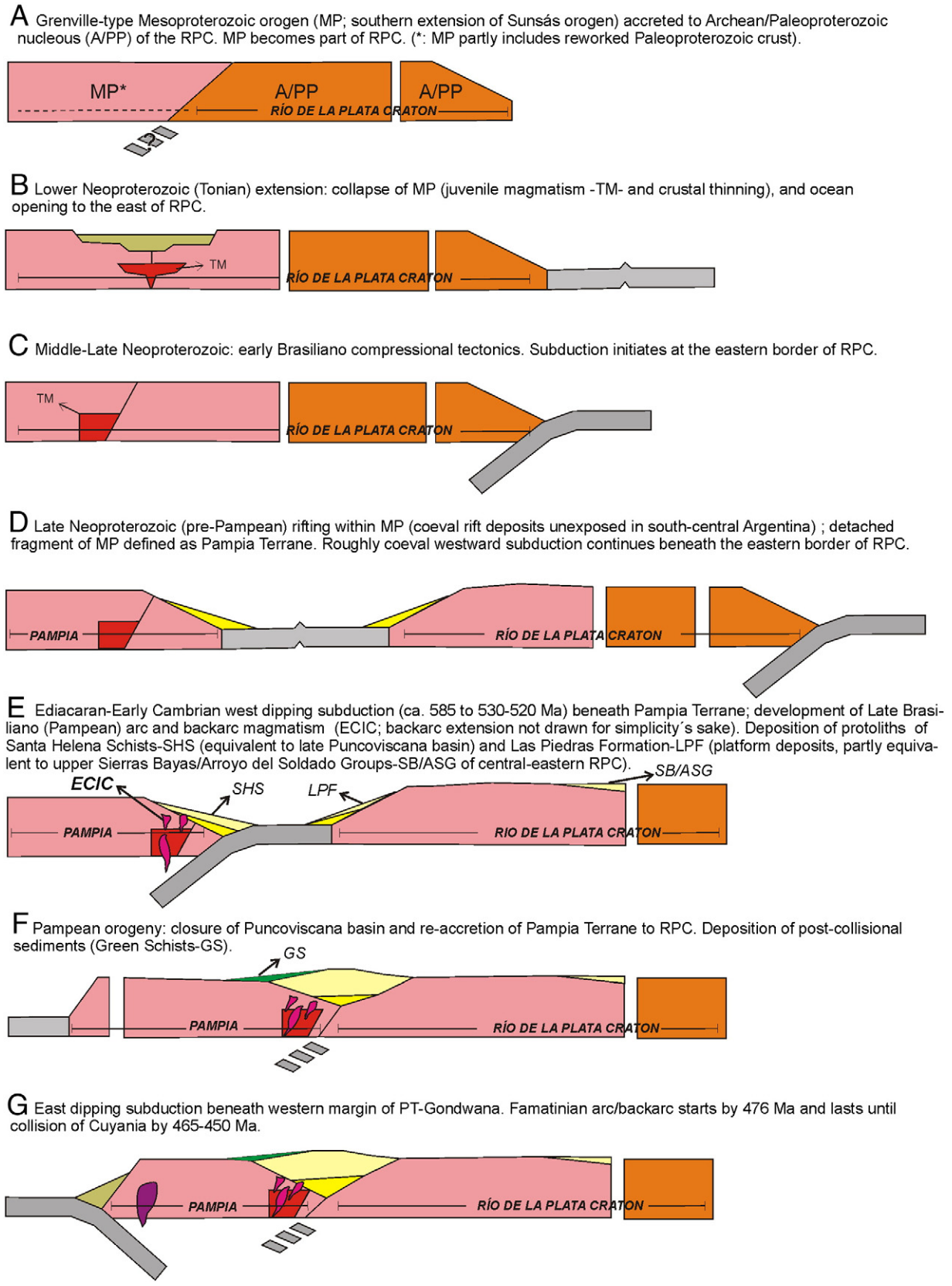

Fig. 7. Pampean orogen in south central Argentina (La Pampa province), and broader tectonic evolution from Mesoproterozoic to Ordovician. Indicated geochronological data, as obtained by the present authors; age 585 Ma, after Schwartz et al. (2008). See also Fig. 8, Zappettini et al. (2010) References: ECIC: El Carancho Igneous Complex; RPC: Río de la Plata craton.

7.4. The configuration of the Rio de la Plata craton and the Pampia terrane

Inherent to our model for the Pampean orogen is that the Río de la Plata craton formed part of Rodinia, although, admittedly, there are big discrepancies between the different Rodinia configurations, some of which would consider that the Río de la Plata craton (and a few other continental fragments) was never part of this supercontinent (e.g. Cordani et al., 2010, and references therein), whereas others (e.g. Li et al., 2008, and references therein) do include this craton.

Recently, based on geological grounds, Frimmel et al. (2010) have envisaged the Rio de la Plata and Kalahari cratons juxtaposed already during the formation of Rodinia at the end of the Mesoproterozoic – the Brazilides Ocean would have opened up later along this Mesoproterozoic suture – , a scenario that would agree with the configuration presented by Li et al. (2008).

Also recently, based on the existence of significant Mesoproterozoic tectonic reworking, magmatism and sedimentation in the Rio de la Plata craton, Gaucher et al. (2010) have suggested that the Rio de la Plata craton was part of Rodinia, where it would have been located at its 'heart', fringed by Mesoproterozoic belts separating it from Laurentia and the Kalahari craton, hence filling a gap indicated by paleomagnetic data between the latter two continental blocks (e.g. Jacobs et al., 2008).

The latter arguments go beyond the scope of the present article, and this last segment of the Discussion is, instead, concerned with the actual configuration of the Río de la Plata craton and Pampia terrane. In this regards, it is important to note that: a) the Paleo-Mesoproterozoic Hf model ages obtained by the present authors both on magmatic zircons from Lower Paleozoic magmatic units and on detrital zircons from Neoproterozoic–Early Cambrian cover sequences in La Pampa province (see Table 4), b) the increased relative abundance of Mesoproterozoic detrital zircons in the Neoproterozoic metasedimentary rocks of the Rio de la Plata craton towards the west of the craton (Gaucher et al., 2008; Blanco et al., 2009) and c) the Mesoproterozoic Nd model ages of the Cambrian igneous basement of Sierra de la Ventana (i.e. immediately southwest of the Rio de la Plata craton basement exposures of Tandilia; Rapela et al., 2003), indicate that during the depositional age of the Rio de la Plata craton supracrustal sequences, a Mesoproterozoic orogen (southern continuation of the Sunsás orogen of SW Amazon) was located at the western border of the Rio de la Plata craton (see also Fig. 17, in Gaucher et al., 2008, and Fig. 6, in Aceñolaza and Toselli, 2009) and acted partly as a source for these supracrustal sequences (and also partly as topographic barrier, depending on the depocenters' locations; e.g. Las Piedras Formation).

Hence, we regard the Rio de la Plata craton to have originally encompassed both: 1) an Archean to Paleoproterozoic nucleus where the Archean zones are less common and the Paleoproterozoic (mainly Rhyacian) zones predominate, and 2) an outer Mesoproterozoic belt accreted to the old nucleus (see also Zappettini et al., 2010), similarly to the Amazon, Kalahari and Congo cratonic nuclei, which are surrounded by Mesoproterozoic (magmatic arcs) terranes/orogens developed during the amalgamation of Rodinia, and that are regarded to form part of these cratons (e.g. Santos et al., 2000; Santos, 2003; De Waele et al., 2008; Jacobs et al., 2008). In this tectonic context, a fragment of the outer Mesoproterozoic belt of the Rio de la Plata craton – and some Rio de la Plata craton Paleoproterozoic crustal material as well – , would have later been rifted away from the Rio de la Plata craton nucleus – sometime prior to 600 Ma – , defining the Pampia terrane. Note that in our concept (see also Chernicoff et al., 2010c), the Pampia terrane does not equal the Mesoproterozoic belt or orogen, as proposed by Ramos et al. (2010), since part of this orogen would have remained as part of the Rio de la Plata craton. This pre-600 Ma extensional event would have given rise to the Puncoviscana basin (northern Sierras Pampeanas and Sierra de Córdoba, Argentina), whose late-stage equivalent at the latitude of La Pampa province is regarded to be represented by the Santa Helena Schist (Zappettini et al., 2010). The detachment of the Pampia terrane from the western border of the Rio de la Plata craton would, in turn, have been roughly coeval with the inferred westward subduction of the Adamastor Ocean lithosphere beneath the eastern border of the Rio de la Plata craton (see e.g. Silva et al., 2005, and references therein). These two coeval events would coincide with the late stage of the Rodinia break-up which, in turn, partly overlaps the timing of Western Gondwana amalgamation.

The Pampia terrane would have been re-accreted to the Rio de la Plata craton during the Early Cambrian Pampean orogeny (see also, e.g. Rapela et al., 1998), which would form part of the more extensive Araguaia-Paraguay-Pampean orogeny, considered to represent a major event shaping West Gondwana (Trindade et al., 2006; Heilbron et al., 2008; Tohver et al., 2010, 2011) during the final stage of Gondwana amalgamation at ca 530–520 Ma. In this context, the El Carancho Igneous Complex pertains to the arc-backarc magmatism related to the aforementioned accretion.

Supplementary materials related to this article can be found online at doi:10.1016/j.gr.2011.04.007.

Acknowledgments

This work received financial support from Research Grant PIP-11220090100181 (CONICET, Council for Scientific and Technical Research of Argentina). The Geological Survey of Argentina (SEGEMAR) provided logistical support and geophysical data. G. Cozzi (INTEMIN-SEGEMAR) carried out the X-ray diffraction analyses of samples 131BF and 131BF2. Two anonymous reviews helped improve an earlier version of the manuscript.

References

Aceñolaza, F.G., Toselli, A., 2009. The Pampean Orogen: Ediacaran–Lower Cambrian evolutionary history of central and northwest region of Argentina. In: Gaucher, C., Sial, A.N., Halverson, G.P., Frimmel, H.E. (Eds.), Neoproterozoic–Cambrian Tectonics, Global Change and Evolution: a focus on southwestern Gondwana. Developments in Precambrian Geology, 16. Elsevier, pp. 239–254.

Adams, Ch.J., Miller, H., Toselli, A., Griffin, W.L., 2008. The Puncoviscana Formation of northwest Argentina: U–Pb geochronology of detrital zircons and Rb–Sr metamorphic ages and their bearing on its stratigraphic age, sediment provenance and tectonic setting. Neues Jahrbuch für Geologie und Paläontologie Abhandlungen 247, 341–352.

Allègre, C.J., Dupré, B., Levin, E., 1986. Thorium/uranium ratio of the Earth. Chemical Geology 56, 219.

Augustsson, C., Münker, C., Bahlburg, H., Fanning, C.M., 2006. Provenance of late Palaeozoic metasediments of the SW South American Gondwana margin: a combined U–Pb and Hf-isotope study of single detrital zircons. Journal of the Geological Society 163, 983–995.

Bailey, E.H., Blake, M.C., 1974. Major chemical characteristics of Mesozoic Coast Range ophiolite in California. Journal of Research of the U.S. Geological Survey 2, 637–656.

Blanco, G., Rajesh, H.M., Gaucher, C., Germs, G.J.B., Chemale Jr., F., 2009. Provenance of the Arroyo del Soldado Group (Ediacaran to Cambrian, Uruguay): implications for the paleogeographic evolution of southwestern Gondwana. Precambrian Research 171, 57–73.

Blichert-Toft, J., Albarède, F., 1997. The Lu–Hf isotope geochemistry of chondrites and the evolution of the mantle–crust system. Earth Planetary Science Letters 148, 243–258.

Booker, J.R., Favetto, A., Pomposiello, M.C., 2004. Low electrical resistivity associated with plunging of the Nazca flat slab beneath Argentina. Nature 249, 399–403.

Chernicoff, C.J., Zappettini, E., 2004. Geophysical evidence for terrane boundaries in south-central Argentina. Gondwana Research 8, 1105–1116.

Chernicoff, C.J., Zappettini, E.O., 2007. La cuenca paleozoica de Arizona, sudeste de San Luis, Argentina: extensión austral de la cuenca de Paganzo. Revista de la Asociación Geológica Argentina 62, 321–324.

Chernicoff, C.J., Santos, J.O.S., Zappettini, E.O., McNaughton, N.J., 2007. Esquistos del Paleozoico Inferior en la cantera Green, sur de San Luis, Argentina: edades U–Pb SHRIMP e implicancias geodinámicas. Revista de la Asociación Geológica Argentina 62, 154–158.

Chernicoff, C.J., Zappettini, E.O., Santos, J.O.S., Beyer, E., McNaughton, N.J., 2008a. Foreland basin deposits associated with Cuyania terrane accretion in La Pampa province, Argentina. Gondwana Research 13, 189–203.

Chernicoff, C.J., Santos, J.O.S., Zappettini, E.O., McNaughton, N.J., 2008b. U–Pb SHRIMP dating of the Famatinian (Lower Paleozoic) metamorphism in La Pampa province, Argentina. VI South American Symposium on Isotope Geology. Digital Proceedings.

Chernicoff, C.J., Santos, J.O.S., Zappettini, E.O., McNaughton, N.J., 2008c. Zircon U–Pb SHRIMP dating of the Lower Paleozoic paraschists at Sierra de Lonco Vaca, La Pampa province, Argentina. VI South American Symposium on Isotope Geology. Digital Proceedings.
Chernicoff, C.J., Santos, J.O.S., Zappettini, E.O., Villar, L.M., McNaughton, N.J., 2008d. Zircon U–Pb SHRIMP dating of the Lower Paleozoic La Pampa belt of metagabbros, Argentina. VI South American Symposium on Isotope Geology. Digital Proceedings.
Chernicoff, C.J., Zappettini, E.O., Villar, L.M., Chemale, F., Hernández, L., 2009. The belt of metagabbros of La Pampa: Lower Paleozoic back-arc magmatism in south-central Argentina. Journal of South American Earth Sciences 28, 383–397.
Chernicoff, C.J., Zappettini, E.O., Santos, J.O.S., Allchurch, S., McNaughton, N.J., 2010a. The southern segment of the Famatinian magmatic arc, La Pampa province, Argentina. Gondwana Research 17, 662–675.
Chernicoff, C.J., Zappettini, E.O., Santos, J.O.S., Belousova, E., McNaughton, N.J., 2010b. SHRIMP U–Pb ages and Hf isotope composition of Las Piedras Formation (Ediacaran–Lower Cambrian), southern La Pampa Province, Argentina. VII South American Symposium on Isotope Geology. Brasilia. Digital Proceedings, Brasilia.
Chernicoff, C.J., Zappettini, E.O., Santos, J.O.S., 2010c. Pampia: a fragment of the authochtonous Mesoproterozoic orogen of western Río de la Plata craton. Its detachment during Rodinia's break-up, and re-accretion during Gondwana's amalgamation. GeoSur 2010. : Special Session: “Rodinia in South America”. Digital Proceedings, Mar del Plata.
Chernicoff, C.J., Zappettini, E.O., Santos, J.O.S., 2011a. Determinaciones isotópicas de hafnio en los metagabros famatinianos de Valle Daza, provincia de La Pampa. Implicancias sobre la existencia de un magmatismo toniano (Neoproterozoico Inferior) en el sustrato de la región centro-austral argentina. 18 Congreso Geológico Argentino. Digital Proceedings, Neuquén.
Chernicoff, C.J., Zappettini, E.O., Santos, J.O.S., Belousova, E., McNaughton, N.J., 2011b. Hf isotope determinations on Paleozoic metaigneous rocks in La Pampa province. Implications for the occurrence of juvenile Early Neoproterozoic (Tonian) magmatism in south-central Argentina. Journal of South American Earth Sciences DOI:10.1016/j.jsames.2011.04.005.
Chew, D.M., Magna, T., Kirkland, C.L., Miskovic, A., Cardona, A., Spikings, R., Schaltegger, U., 2008. Detrital zircon fingerprint of the Proto-Andes: evidence for a Neoproterozoic active margin? Precambrian Research 167, 186–200.
Collo, G., Astini, R.A., Cawood, P.A., Buchan, C., Pimentel, M., 2009. U–Pb detrital zircon ages and Sm–Nd isotopic features in low-grade metasedimentary rocks of the Famatina belt: implications for late Neoproterozoic–early Palaeozoic evolution of the proto-Andean margin of Gondwana. Journal of the Geological Society 166, 303–319.
Cordani, U.G., Sato, K., Teixeira, W., Tassinari, C.C.G., Basei, M.A.S., 2000. Crustal evolution of the South American platform. In: Cordani, U.G., Milani, E.J., Thomaz-Filho, A., y Campos, D.A. (Eds.), Tectonic Evolution of South America, 31st International Geological Congress, Río de Janeiro, pp. 19–40.
Cordani, U.G., Fraga, L.M., Colombo, N.R., Tassinari, C.G., Brito-Neves, B.B., 2010. On the origin and tectonic significance of the intra-plate events of Grenvillian-type age in South America: a discussion. Journal of South American Earth Sciences 29, 143–159.
Dalla Salda, L., de Barrio, R.E., Echeveste, H.J., Fernández, R.R., 2005. El basamento de las Sierras de Tandilia. 16 Argentine Geological Congress, Proceedings, 1, pp. 31–50. La Plata.
De Waele, B., Johnson, S.P., Pisarevsky, S.A., 2008. Palaeoproterozoic to Neoproterozoic growth and evolution of the eastern Congo Craton: its role in the Rodinia puzzle. Precambrian Research 160, 127–141.
Elliot, T., Zindler, A., Bourdion, B., 1999. Exploring the kappa conundrum: the role of recycling in the lead isotope evolution of the mantle earth and planetary. Science letters 169, 129–145.
Escayola, M.P., Pimentel, M.M., Armstrong, R., 2007. Neoproterozoic backarc basin: Sensitive high-resolution ion microprobe U–Pb and Sm–Nd isotopic evidence from the Eastern Pampean Ranges, Argentina. Geology 35, 495–498.
Espejo, P.M., Silva Nieto, D.G., 1996. Puelches. Programa Naiconal de Cartas Geológicas 1:250.000. Dirección Nacional del Servicio Geológico. Boletín, 216, pp. 1–35. Buenos Aires.
Essex, R.M., Gromet, L.P., 2000. U–Pb dating of prograde and retrograde titanite growth during the Scandian orogeny. Geology 28 (5), 419–422.
Frimmel, H.E., Basei, M.S., Gaucher, C., 2010. Neoproterozoic geodynamic evolution of SW-Gondwana: a southern African perspectiva. International Journal of Earth Sciences DOI:10.1007/s00531-010-0571-9.
Frost, B.R., Chamberlain, K.R., Schumacher, J.C., 2000. Sphene (titanite): phase relations and role as a geochronometer. Chemical Geology 172, 131–148.
Galer, S.J.G., O'Nions, R.K., 1985. Residence time for thorium, uranium, and lead in the mantle with implications for mantle convection. Nature 316, 778–782.
Gaucher, C., Poiré, D., Peral, L., Chiglino, L., 2005. Litoestratigrafía, Bioestratigrafía y correlaciones de las sucesiones sedimentarias del Neoproterozoico–Cámbrico del Cratón del Río de la Plata (Uruguay y Argentina). Latin American Journal of Sedimentology and Basin Analysis 12, 145–160.
Gaucher, C., Finney, S., Poiré, D., Valencia, V., Grove, M., Blanco, G., Paoumukaghlian, L., Peral, L., 2008. Detrital zircon ages of Neoproterozoic sedimentary successions in Uruguay and Argentina: insights into the geological evolution of the Río de la Plata Craton. Precambrian Research 167, 150–170.
Gaucher, C., Frei, R., Chemale Jr., F., Frei, D., Bossi, J., Martínez, G., Chiglino, L., Cernuschi, F., 2010. Mesoproterozoic evolution of the Río de la Plata Craton in Uruguay: at the heart of Rodinia? International Journal of Earth Sciences. doi:10.1007/s00531-010-0562.
Gemelli, M., Rocchi, S., Di Vincenzo, G., Petrelli, M., 2009. Accretion of juvenile crust at the Early Palaeozoic Antarctic margin of Gondwana: geochemical and geochronological evidence from granulite xenoliths. Terra Nova 21, 151–161.
Gómez Peral, L., Poiré, D.G., Strauss, H., Zimmermann, U., 2007. Chemostratigraphy and diagenetic constraints on Neoproterozoic carbonate successions from the Sierras Bayas Group, Tandilia System, Argentina. Chemical Geology 237, 109–128.
Green, T.H., 1977. Garnet in silicic liquids and its possible use as a P–T indicator. Contribution to Mineralogy and Petrology 65, 59–67.
Griffin, W.L., Pearson, N.J., Belousova, E.A., Jackson, S.R., van Achterbergh, E., O'Reilly, S.Y., Shee, S.R., 2000. The Hf isotope composition of cratonic mantle: LAM-MC-ICPMS analysis of zircon megacrysts in kimberlites. Geochimica et Cosmochimica Acta 64, 133–147.
Griffin, W.L., Belousova, E.A., Shee, S.R., Pearson, N.J., O'Reilly, S.Y., 2004. Archean crustal evolution in the northern Yilgarn Craton: U–Pb and Hf-isotope evidence from detrital zircons. Precambrian Research 131, 231–282.
Griffin, W.L., Pearson, N.J., Belousova, E.A., Saeed, A., 2007. Reply to “Comment to short-communication ‘Comment: Hf-isotope heterogeneity in zircon 91500’ by W.L. Griffin, N.J. Pearson, E.A. Belousova and A. Saeed (Chemical Geology 233 (2006) 358–363)” by F. Corfu. Chemical Geology 244, 354–356.
Hauser, N., Matteini, M., Omarini, R.H., Pimentel, M.M., 2010a. Combined U–Pb and Lu–Hf isotope data on turbidites of the Paleozoic basement of NW Argentina and petrology of associated igneous rocks: Implications for the tectonic evolution of western Gondwana between 560 and 460 Ma. Gondwana Research. doi:10.1016/j.gr.2010.04.002.
Hauser, N., Matteini, M., Omarini, R.H., Pimentel, M.M., 2010b. Combined U–Pb and Lu–Hf isotopes on turbidites from the basement of NW Argentina: maximum and minimum ages and implications for the tectonic evolution of western Gondwana between 560 and 460 Ma. VII South American Symposium on Isotope Geology. Digital Proceedings.
Heilbron, M., Valeriano, C.M., Tassinari, C.C.G.-, Almeida, J., Tupinambá, M., Siga Jr., O., Trouw, R., 2008. Correlation of Neoproterozoic terranes between the Ribeira Belt, SE Brazil and its African counterpart: comparative tectonic evolution and open questions. In: Pankhurst, R.J., Trouw, R.A.J., De Brito Neves, B.B., De Wit, M.J. (Eds.), West Gondwana: Pre-Cenozoic Correlations Across the South Atlantic Region. : Special Publications, 294. Geological Society, London, pp. 211–237.
Irvine, T.N., Baragar, W.R.A., 1971. A guide to the chemical classification of the common volcanic rocks. Canadian Journal of Earth Sciences 8, 523–548.
Jacobs, J., Pisarevsky, S., Thomas, R.J., Becker, T., 2008. The Kalahari Craton during the assembly and dispersal of Rodinia. Precambrian Research 160, 142–158.
Kemp, A.I.S., Hawkesworth, C.J., Foster, G.L., Paterson, B.A., Woodhead, J.D., Hergt, J.M., Gray, C.M., Whitehouse, M.J., 2007. Magmatic and crustal differentiation. History of granitic rocks from Hf–O isotopes in zircon. Science 315, 980–983.
Kraemer, P.E., Escayola, M.P., Martino, R.D., 1995. Hipótesis sobre la evolución tectónica neoproterozoica de las Sierras Pampeanas de Córdoba (30°40′–32°40′). Revista Asociación Geológica Argentina 50, 47–59.
Lagorio, S., Zappettini, E.O., Chernicoff, C.J., 2008. Stock Estancia El Trabajo: evidencias de magmatismo alcalino triásico en la provincia de La Pampa. 17 Congreso Geológico Argentino, Actas, pp. 1363–1364. San Salvador de Jujuy.
Li, Z.X., Bogdanova, S.V., Collins, A.S., Davidson, A., De Waele, B., Ernst, R.E., Fitzsimons, I.C.W., Fuck, R.A., Gladkochub, D.P., Jacobs, J., Karlstrom, K.E., Lu, S., Natapov, L.M., Pease, V., Pisarevsky, S.A., Thrane, K., Vernikovsky, V., 2008. Assembly, configuration and break-up of Rodinia: a synthesis. Precambrian Research 160, 179–210.
Lira, R., Millone, H.A., Kirschbaum, A.M., Moreno, R.S., 1997. Calc–alkaline arc granitoid activity in the Sierra Norte-Ambargasta Ranges, Central Argentina. Journal of South American Earth Sciences 10, 157–177.
López Gamundi, O.R., Conaghan, P., Rossello, E.A., Cobbold, P.R., 1995. The Tunas Formation (Permian) in the Sierras Australes Foldbelt, East-Central Argentina: evidence of syntectonic sedimentation in a Varisican foreland basin. Journal of South American Earth Sciences 8, 129–142.
Ludwig, K.R., 2001. Squid 1.02: A Users Manual. : Special Publication, 2. Berkeley Geochronology Centre. 19 p.
Ludwig, K.R., 2003. Isoplot 3.00, a geochronological tool-kit for Excel. : Special Publication, 4. Berkely Geochronology Center. 67 p.
Macdonald, G.A., Katsura, T., 1964. Chemical composition of Hawaiian lavas. Journal of Petrology 5, 82–133.
Meschede, M., 1986. A method of discriminating between different types of mid-ocean ridge basalts and continental tholeiites with the Nb–Zr–Y diagram. Chemical Geology 56, 207–218.
Miller, C.F., Stoddard, E.F., 1980. The role of manganese in the paragenesis of magmatic garnet: an example from the Old Woman–Piute range, California. Journal of Geology 89, 233–246.
Mohammad, Y.O., Maekawa, H., 2008. Origin of titanite in metarodingite from the Zagros Thrust Zone, Iraq. American Mineralogist 93 (7), 1133–1141.
Mosquera, A., Ramos, V.A., 2006. Intraplate deformation in the Neuquén Embayment. In: Kay, S.M., Ramos, V.A. (Eds.), Evolution of an Andean margin: A tectonic and magmatic view from the Andes to the Neuquén Basin (35°–39°S lat). : Special Paper, 407. Geological Society of America, pp. 97–123.
Pankhurst, R.J., Rapela, C.W., Fanning, C.M., Márquez, M., 2006. Gondwanide continental collision and the origin of Patagonia. Earth-Science Reviews 76, 235–257.
Pearce, J.A., 1982. Trace element characteristics of lavas from destructive plate boundaries. In: Thorpe, R.S. (Ed.), Andesites, pp. 525–548.
Pearce, J.A., Cann, J.R., 1973. Tectonic setting of basic volcanic rocks using Ti, Zr and Y. Earth and Planetary Science Letters 19, 290–300.
Pearce, J.A., Harris, N.B.W., Tindle, A.G., 1984. Trace element discrimination diagrams for the tectonic interpretation of granitic rocks. Journal of Petrology 25, 956–983.
Poiré, D.G., Spalletti, L.A., 2005. La cubierta sedimentaria precámbrica/paleozoica inferior del Sistema de Tandilla. In: De Barrio, R.E., Etcheverry, R.O., Caballé, M.F.,

Llambías, E.J. (Eds.), Geología y Recursos Minerales de la provincia de Buenos Aires: 16 Congreso Geológico Argentino. Relatorio, pp. 51–68.
Raimondo, T., Collins, A.S., Hand, M., Walker-Hallam, A., Smithies, R.H., Evins, P.M., Howard, H.M., 2009. Ediacaran intracontinental channel flow. Geology 37, 291–294.
Ramé, G.A., Miró, R.C., 2010. Estudio gravimétrico del borde occidental del cratón del Río de la Plata. 6 Congreso Uruguayo de Geología. Digital Proceedings, Minas Lavalleja, Uruguay. No. 71.
Ramos, V.A., 1988. Late Pretorozoic–Early Paleozoic of South America—a collisional history. Episodes 11, 168–174.
Ramos, V.A., Vujovich, G., Martino, R., Otamendi, J., 2010. Pampia: a large cratonic block missing in the Rodinia supercontinent. Journal of Geodynamics 50, 243–255.
Rapela, C.W., Pankhurst, R.J., Casquet, C., Baldo, E., Saaverdra, J., Galindo, C., Fanning, C.M., 1998. The Pampean Orogeny of the southern Proto-Andean: Cambrian continental collision in the Sierras de Córdoba. In: Pankhurst, R.J., Rapela, C.W. (Eds.), The Proto-Andean Margin of Gondwana. : Special Publication. Geological Society of London, pp. 181–217.
Rapela, C.W., Pankhurst, R.J., Fanning, C.M., Grecco, L.E., 2003. Basement evolution of the Sierra de la Ventana Fold Belt: new evidence for Cambrian continental rifting along the southern margin of Gondwana. Journal of the Geological Society 160, 613–628.
Rapela, C.W., Pankhurst, R.J., Casquet, C., Fanning, C.M., Baldo, E., González-Casado, J.M., Galindo, C., y Dahlquist, J., 2007. The Río de la Plata craton and the assembly of SW Gondwana. Earth-Science Reviews 83, 49–82.
Rizzotto, G.J., Chemale, F., Lima, E.F., Van Schmus, W.R., Fetter, A., 1999. Dados isotópicos Sm–Nd and U–Pb das rochas da sequência metavulcanossedimentar Nova Brasilândia (SMNB)—RO. Sociedade Brasileira de Geologia, Núcleo Norte, Simpósio de Geologia da Amazônia. : Boletim de Resumos Expandidos, 6. Companhia de Pesquisa de Recursos Minerais, Manaus, Amazonas, pp. 490–493.
Rocchi, S., Bracciali, L., Di Vincenzo, G., Gemelli, M., Ghezzo, C., 2010. Arc accretion to the early Paleozoic Antarctic margin of Gondwana in Victoria Land. Gondwana Research. doi:10.1016/j.gr.2010.08.001.
Santos, J.O.S., 2003. Geotectônica dos escudos das Guianas e Brasil-Central. In: Bizzi, L.A., Schobbenhaus, C., Vidotti, R.M., Gonçalves, J.H. (Eds.), Geologia, tectônica e recursos minerais do Brasil. Companhia de Pesquisa de Recursos Minerais, Brasília, pp. 169–226. 674 pp.
Santos, J.O.S., Hartmann, L.A., Gaudette, H.E., Groves, D.I., McNaughton, N.J., y Flecher, I.R., 2000. A new understanding of the provinces of the Amazon Craton based on integration of field mapping and U–Pb and Sm–Nd geochronology. Gondwana Research 3, 489–506.
Santos, J.O.S., Hartmann, L.A., Bossi, J., Campal, N., Schipilov, A., Piñeiro, McNaughton, N.J., 2003. Duration of the Trans-Amazonian Cycle and its correlation within South America based on U–Pb SHRIMP geochronology of the La Plata craton, Uruguay. International Geology Review 45, 27–48.
Santos, J.O.S., Rizzotto, G.J., Potter, P.E., McNaughton, N.J., Matos, R.S., Hartmann, L.A., Chemale Jr., F., Quadros, M.E.S., 2008. Age and autochthonous evolution of the Sunsás Orogen inWest Amazon Craton based on mapping and U–Pb geochronology. Precambrian Research 165, 120–152.
Scherer, E., Münker, C., Mezger, K., 2001. Calibration of the Lutetium-Hafnium clock. Science 293, 683–687.
Schwartz, J.J., Gromet, L.P., 2004. Provenance of Late Proterozoic–early Cambrian basin, Sierras de Córdoba, Argentina. Precambrian Research 129, 1–21.
Schwartz, J.J., Gromet, L.P., Miró, R., 2008. Timing and duration of the calcalkaline arc of the Pampean Orogeny: implications for the Late Neoproterozoic to Cambrian evolution of Western Gondwana. Journal of Geology 116, 39–61.
SEGEMAR, 2005. Aeromagnetic survey of La Pampa, Argentina: digital data. Servicio Geológico-Minero Argentino.
Silva, L.C., McNaughton, N.J., Armstrong, R., Hartmann, L.A., Fletcher, I.R., 2005. The neoproterozoic Mantiqueira Province and its African connections: a zircon-based U–Pb geochronologic subdivision for the Brasiliano/Pan-African systems of orogens. Precambrian Research 36, 203–240.
Spagnuolo, C.M., Rapalini, E., Astini, R.A., 2011. Assembly of Pampia to the SW Gondwana margin: a case of strike–slip docking? Gondwana Research. doi:10.1016/j.gr.2011.02.004.
Taylor, S.R., McLennan, S.M., 1985. The Continental Crust: Its Composition and Evolution. Blackwell, Oxford. 312 pp.
Tickyj, H., Dimieri, L.V., Llambías, E.J., Sato, A.M., 1997. Cerro Los Viejos (38° 28′ S–64° 26′ O): cizallamiento dúctil en el sudeste de La Pampa. Revista Asociación Geológica Argentina 52, 311–321.
Tickyj, H., Llambías, E.J., Sato, A.M., 1999. El basamento cristalino de la región sur-oriental de la provincia de La Pampa: Extensión austral del Orógeno Famatiniano de Sierras Pampeanas. 14 Congreso Geológico Argentino: Proceedings, 1, pp. 160–163. Salta.
Tohver, E., Trindade, R.I.F., Solum, J.G., Hall, C.M., Riccomini, C., Nogueira, A.C., 2010. Closing the Clymene Ocean and bending a Brasiliano belt: evidence for the Cambrian formation of Gondwana, southeast Amazon craton. Geology 38, 267–270.
Tohver, E., Cawood, P.A., Rossello, E.A., Jourdan, F., 2011. Closure of the Clymene Ocean and formation of West Gondwana in the Cambrian: evidence from the Sierras Australes of the southernmost Rio de la Plata craton, Argentina. Gondwana Research. doi:10.1016/j.gr.2011.04.001.
Trindade, R.I.F., D'Agrella Filho, M.S., Epof, I., Neves, B.B.B., 2006. Paleomagnetism of Early Cambrian Itabaiana mafic dikes (NE Brazil) and the final assembly of Gondwana. Earth and Planetary Science Letters 244, 361–377.
Zappettini, E.O., Chernicoff, C.J., Santos, J.O.S., y McNaughton, N.J., 2010. Los esquistos neoproterozoicos de Santa Helena, provincia de La Pampa, Argentina: edades U–Pb SHRIMP, composición isotópica de hafnio e implicancias geodinámicas. Revista de la Asociación Geológica Argentina 66, 21–37.